UNIVERSITA' DEGLI STUDI DI PADOVA

ÉCOLE NATIONALE SUPÉRIEURE D'ARTS ET MÉTIERS - CAMPUS DE LILLE

Dipartimento di Ingegneria Industriale DII

Laboratoire de Mécanique des Fluides de Lille – Kampé de Fériet

Corso di Laurea Magistrale in Ingegneria Energetica

Active Flow Control in an Axial Compressor: Effect of the Injection Angle

Supervisors:

Prof. Antoine Dazin

Prof. Giorgio Pavesi

Prof. Pierric Joseph

PhD Gabriel Margalida

PhD Alberto Baretter

Giacomo Gatti

1171799

Anno Accademico 2018/2019

Preface

This master thesis, entitled "Active Flow Control in an Axial Compressor: Effect of the Injection Angle", comprises the research carried out at the École Nationale Supérieure d'Arts et Métiers of Lille from March 1, 2019 to August 31, 2019. Professors Antoine Dazin, Giorgio Pavesi, Pierric Joseph and PhD students Gabriel Margalida and Alberto Baretter were supervisors.

The thesis is organized in ten chapters: the first chapter gives the context and the objectives of the research. The second chapter outlines the experimental test bench used. Third and fourth ones describe the data acquisition system and the experimental setup. In the fifth chapter programs used and built up for the data processing are described. In the sixth one, results obtained are presented and discussed. The seventh gives the main conclusions of this thesis work while the eighth discusses the possible future perspectives. Lastly, the ninth contains the references of the work and the tenth an appendix with links to programs used.

Acknowledgements

I wish to thank my supervisors, Professors Antoine Dazin, Giorgio Pavesi and Pierric Joseph for giving me the opportunity to grow personally and professionally trough these six months experience at ENSAM.

I would like also to thank my so-supervisors Gabriel Margalida and Alberto Baretter for teaching me everything, for their patience and time answering my questions and for their support in every moment.

A special thank goes to my girlfriend for her great support, for having pushed me in this experience; I will never be able to say thank you enough.

I wish to thank all the colleagues there; they make me feel part of this big team. Especially Shu Lei, Shing Lei and Guanjang Wang for the beautiful moments spent together everyday.

I would like to say thank you to myself, for never give up, for pushing everyday to do my best, for believing in this experience. I will never forget it! It is a part of me, a great part of me, and will always remember me that dreams are possible.

Abstract

Compressor's technology, particularly axial's one, is affirmed and spread all around the world for its multiple utilities; from aerospace engeneer which is used for example in turbojet engine powering aircrafts, passing through turbogas power plant and up to many others industrial exploitations.

This type of technology is really well known; industries and research labs know perfectly how to manage a compressor and how to make it working properly; changing different rotational speed, changes the compressor characteristic curve and so changes its range operability. They also learn that an axial compressor has an inferior limit where its performances are strongly reduced and where it cannot work properly. So, they always avoid to get closer to this conditions because it won't be safe in many cases.

This inferior limit is due to the *Rotating Stall* and *Surge*, phenomena that researchers know very well. When the overall mass flow rate flowing inside the compressor is reduced too much, it would enter this particular condition where its performances are considerably reduced.

Thinking about rotating stall it's obvious to see it as a limit. For example, in a turbogas power plant, if the power required at the plant is too low, the entire engine would be forced to stop because it couldn't work at so restrictive conditions in which it is compelled to reduce its mass flow rate and so entering rotating stall conditions; or, for example, a turbojet aircraft engine must not to go closer to this conditions otherwise there will be catastrophic consequences.

For these reasons, looking at this particular and ever present problem, it's really important to understand it, how to postpone it (if it is possible) and how to look at warnings the compressor is sending immediately before reaching rotating stall.

Thus, in this way, this experimental thesis work was done; particularly, this study concerns an active control tecnique which enables to postpone rotating stall. It consists in high pressure air injection in the tip part of the blade, where conditions are critical when approaching rotating stall. Moreover, this active control was applied for different injection angle layout in order to determine if there were an optimal injection configuration, and this was about the first part.

The second one, was trying to understand why this is the best configuration; despite several attemps, due to the lack of a mathematical model for this problem, this part was found very hard to do. What was done

to try to get some answer at the question, is to have a look inside the blade stage on what's happening when compressor is reaching rotating stall with the active control on.

Parameters that played an important role were: pressure, injectors number and injection angle. Throughout the whole study it had to be dealt with these three quantities trying to understand how they behave one with the others. Tests were performed in the *Laboratoire de Mecanique des Fluides* in Lille (FR), placed inside the *École Nationale Supérieure d'Arts et Métiers*, on a single stage axial compressor.

This project thesis work is the last part of a PhD thesis work made by a french student, and it stands inside a big research project called *NumERICCS* which stands for Numerical and Experimental Research for Improved Control of Compressor Surge; it is part of french *ANR – Agence Nationale de la Recherche* and involves french universities like *ENSAM* (Lille), *École Centrale* (Lille), *UPMC – Université Pierre et Marie Curie* (Paris), the french aerospace research organization *ONERA*, and of the french aircraft-engine manufacturer *SNECMA*.

List of figures

List of Tables

Riassunto

Questo lavoro è stato un lavoro lungo 6 mesi a partire da Marzo ad Agosto 2019 che l'autore ha svolto come parte del programma "Erasmus + for Traineeship" passato in Francia, a Lille, all'*École Nationale Supérieure d'Arts et Métiers*, all'interno del *Laboratoire de Mecanique des Fluides* situato all'interno della scuola.

La tecnologia del compressore, in particolare quella assiale, è affermata e diffusa in tutto il mondo per le sue molteplici utilità; dall'ingegnere aerospaziale in cui viene utilizzata ad esempio nei motori che spingono gli aeromobili, passando attraverso gruppi turbogas per la produzione di energia elettrica, fino a molti altri sfruttamenti industriali. Questo tipo di tecnologia è davvero ben noto; industrie e laboratori di ricerca sanno perfettamente come gestire un compressore e come farlo funzionare correttamente; a seconda delle esigenze, del carico richiesto o di altri fattori ambientali esterni è possibile, cambiando velocità di rotazione, cambiare la curva caratteristica del compressore e quindi cambiare il suo range di operatività.

È risaputo anche, che un compressore assiale ha un limite inferiore di funzionamento corretto oltre il quale le sue prestazioni sono fortemente ridotte e dove non funziona più correttamente. Pertanto, si evita sempre di avvicinarsi a queste condizioni perchè, in molti casi, potrbbe non risultare sicuro farlo.

Questo limite inferiore viene chiamato Stallo Rotante ed è un fenomeno che i ricercatori conoscono molto bene. Questo si verifica quando la portata totale di massa che scorre all'interno del compressore è troppo ridotta, per cui il compressore entra in questa particolare condizione in cui le sue prestazioni diminuiscono notevolmente. In particolare si formano delle zone tra le pale del compressore in cui l'aria, che normalmente dovrebbe passare attraverso di esse e scorrere a valle dello stesso, rimane bloccata all'interno di questi passaggi e crea delle zone di ricircolo, impedendo alla portata in ingresso di passare attraverso questi spazi e deviandola sulle pale adiacenti. Questo fenomeno si verifica a causa dell'aumento eccessivo dell'angolo di attacco al leading edge del profilo palare.

Pensando allo stallo rotante è ovvio vederlo come un limite. Ad esempio, in una centrale elettrica turbogas, se la potenza richiesta nell'impianto è troppo bassa, l'intero motore sarebbe costretto a fermarsi perché non potrebbe funzionare in condizioni così restrittive in cui è costretto a ridurre la sua portata di massa, entrando così in condizioni di stallo rotante; o, ad esempio, un motore di un velivolo turbojet non deve avvicinarsi a queste condizioni, altrimenti si avranno conseguenze catastrofiche che possono portare anche ad incidente aereo. Per questi motivi, osservando questo particolare e sempre presente problema, è

davvero importante capire come posticiparlo (se possibile), se è possibilie prevederlo e come osservare I segnali di allarme che il compressore invia, immediatamente prima di raggiungere lo stallo rotante.

Pertanto, in questo modo, è stato svolto questo lavoro di tesi sperimentale; in particolare, questo studio ha riguardato una tecnica di controllo attivo che consente di posticipare lo stallo rotante. Consiste nell'iniezione di aria ad alta pressione nella zona della punta della punta del pale, dove le condizioni sono critiche quando ci si avvicina allo stallo rotante. Questo tipo di controllo tramite iniezione di aria ad alta pressione è stato realizzato per mezzo di 40 iniettori disposti a coppie tutto attorno al compressore, 10 mm prima dell'ingresso dell'aria nella sezione rotorica. Tramite questo tipo di controllo, sono stati testati diversi layout dell'angolo di iniezione al fine di determinare se ci fosse una configurazione di iniezione ottimale che permettesse di posticipare, in termini di portata principale che fluisce internamente al compressore. Questo lavoro ha riguardato quindi la prima parte di questa tesi.

La seconda invece, ha riguardato la ricerca della motivazione del perchè quella trovata sia la migliore configurazione possibile per il compressore; tuttavia, nonostante diversi tentativi, a causa della mancanza di un modello matematico in grado di spiegare questo problema, e, per di più, a causa della mancanza di conoscenza della velocità all'uscita da ciascun iniettore, questa parte è stata molto difficile da completare. Quello che è stato fatto per cercare di ottenere una risposta alla domanda, è stato quello di dare un'occhiata all'interno dello stadio di compressione, in particolare su ciò che accade quando il compressore sta raggiungendo lo stallo rotante mentre il sistema di controllo attivo funziona.

I parametri che hanno svolto un ruolo importante durante l'analisi di questo problema sono stati: pressione, numero di iniettori e angolo di iniezione. Durante l'intero studio è stato necessario trattare queste tre quantità cercando di capire come si comportano l'una con l'altra. I test sono stati eseguiti presso il *Laboratoire de Mecanique des Fluides de Lille - LMFL* (FR), collocato all'interno *dell'École Nationale Supérieure d'Arts et Métiers*, su un compressore assiale monostadio.

Questo lavoro di tesi è in realtà l'ultima parte di un lavoro di tesi di dottorato realizzato da uno studente francese la quale si trova all'interno di un grande progetto di ricerca chiamato NumERICCS che sta per Numerical and Experimental Research for Improved Control of Compressor Surge; questo grande progetto fa parte dell'ANR francese (Agence Nationale de la Recherche) e coinvolge università francesi come ENSAM (Lille), École Centrale (Lille), UPMC - Université Pierre et Marie Curie (Parigi), l'organizzazione francese di ricerca aerospaziale ONERA, e quella francese produttore di motori aeronautici SNECMA.

Relativamente poi a quest'opera, è stata pensata in modo da fornire al lettore un'idea chiara sul percorso e sui test svolti durante tutta l'esperienza; viene dapprima presentato il problema e come finora è stato trattato e affrontato; successivamente viene descritto il sistema del laboratorio, con il compressore e il sistema di controllo attivo; poi viene presentato il sistema di acquisizione dei dati utilizzato; da questo poi si è passati a descrivere il set up degli esperimenti, le varie configurazioni utilizzate, i vari layout testati; di seguito a questo si è passati alla descrizione dei programmi utilizzati e anche creati per poter trattare, organizzare ed elaborare tutti i dati raccolti durante la fase sperimentale; infine vengono presentati i risultati ottenuti tramite molteplici grafici che hanno permesso di comparare le diverse configurazioni utilizzate durante i test. Alla fine vengono riportate le conclusioni a cui si è giunti, quelle che potrebbero essere le prospettive future, insieme ad una appendice dove vengono riportati i tre grossi programmi Matlab utilizzati nella fase di elaborazione dei dati.

Tre sono state le macroaree in cui può essere suddiviso questo lavoro:

- Nella prima parte dell'esperienza il lavoro svolto nelle prime settimane ha riguardato essenzialmente la documentazione riguardo al problema e la ricerca bibliografica di articoli e altro materiale scentifico che potesse rendere più completo il problema da affrontare. Unitamente a questo, l'autore ha preso dimestichezza con il compressore, con il sistema di acquisizione e con il sistema di iniezione compiendo dei semplici test, alcuni dei quali utili ad uno dei dottorandi per ultimare il suo lavoro di tesi;

- Nella seconda parte sono stati fatti I test per poter trovare la configurazione ottimale allo specifico compressore; in particolare l'autore ha manualmente cambiato la configurazione di iniezione, svolto I test, e, successivamente, analizzato I dati tramite un programma Matlab datogli dallo stesso dottorando. Per poter poi confrontare configurazioni diverse, egli ha dovuto costruirne uno che raccogliesse tutti I dati rilevanti per ciascun test fatto, organizzandoli in modo da ottenere dei grafici comparativi. All'interno di questa seconda fase l'autore ha presentato il suo lavoro finora svolto al gruppo di ricerca all'interno del *LMFL*;

Infine nell'ultimissima parte, l'autore ha fatto dei nuovi test, sulle stesse precedenti configurazioni dell'angolo di iniezione, in modo da valutare il comportamento dell'aria all'interno della sezione palare, analizzando I dati di pressione ottenuti, tramite un altro programma Matlab sempre sviluppato dal medesimo dottorando.

Summary

14

1 INTRODUCTION

Axial compressor is a worldwide very well known technology; there are several applications where it is used like for example gas turbines power plant and jet aircraft engine. One of the most problematic thing affecting compressor is the rotating stall; but what is it?

"Rotating stall (propagating stall) consists of large stall zones covering several blade passages and propagates in the direction of the rotation and at some fraction of rotor speed." (Boyce, 2012)
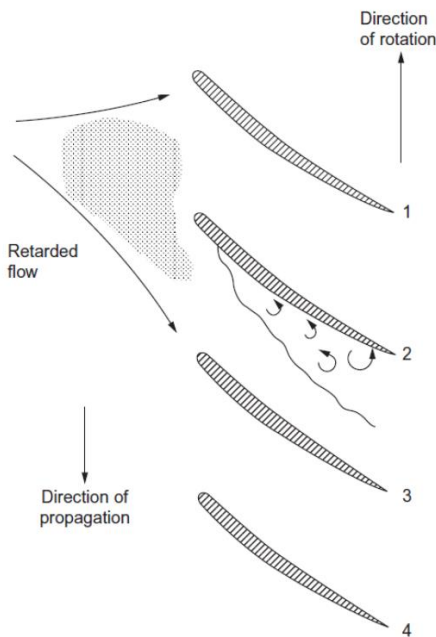
Figure 1: Rotating Stall appearing

Practically Rotating Stall is a phenomenom involving several blades pitch in which mass flow rate cannot pass inside because they are all blocked and compressor performance abruptly decrease (Day, 2015)(Li, Du, Nie, & Zhang, 2019). Once a blade reaches rotating stall, soon the inlet mass flow is deflected: some blades will be unloaded and rapidly facing flow blockage due to vortexes, while some others will be overloaded finding a positive situation.

Considering a general compressor, it is possible to plot its characteristic curve as shown in Figure 2; usually what represented is the pressure gain (or pressure ratio or pressure coefficient) as a function of mass flow rate (or flow coefficient). Compressor has a maximum mass flow rate at which it can run and a minimum one before loosing its performances; passing from its maximum mass flow rate to its minimum one,

compressor increases its performances in terms of pressure it is able to give to mass flow rate. This happens until it reaches rotating stall condition, where its performances immediately drops both in terms of pressure and mass flow rate.

Rotating stall has been studied deeply; some mathemathical models were obtained to describe the way a compressor goes into rotating stall and behaves when it is in these conditions (Greitzer, 1976b, 1976a). In these papers, it's also presented the problem that Rotating Stall could lead, which is Surge. It is a particular phenomenon happening when downstream compressor stage there's a plenum (like a combustion chamber for example), so there might be a pressure which is greater than the atmospheric one and this could lead to the mass flow coming back from the plenum to compressor inlet section. Anyway, this has never happen during this thesis work and these two papers (Greitzer, 1976b, 1976a) and also (Day, 2015; Li et al., 2019) were taken as a base to better understand Rotating Stall problem and the work that has been doing on it.

One of the way to delay rotating stall is to use active flow injection; it consists in air injection localized at the tip of the blade (Suder, Hathaway, Thorp, Strazisar, & Bright, 2002)(Beheshti, Ghorbanian, Farhanieh, Teixeira, & Ivey, 2008)(Mushtaq, Parvez, Ahmad, & Khan, 2012)(Taghavi-Zenouz & Ababaf Behbahani, 2018) (Li, Lin, Tong, Nie, & Chen, 2014) (Lu, Chu, Zhu, & Tong, 2006)(WANG, CHU, ZHANG, & KUANG, 2017)(Nie, Tong, Geng, Zhu, & Huang, 2007)(Nie, Xu, Cheng, & Chen, 2002)(Salunkhe, Reddy, & Pradeep, 2009). Air injected allows to push vortexes, created by leading edge fluid separation, downstream avoiding blade pitch blockage and so Rotating Stall appearance.

The compressor used in tests is an axial, single blade stage one; its characteristics are shown in Table 1; it is provided by a series of injectors coupled in pair, and placed immediately in front of it; injectors configurations, pressure and injection angle can be changed (Guinet, Inzenhofer, & Gümmer, 2016).

So, starting from this point, it was looking for the best injection angle configuration after reading some papers talking about it (Kefalakis & Papailiou, 2008)(Kefalakis & Papailiou, 2007)(Behnken, 1997).
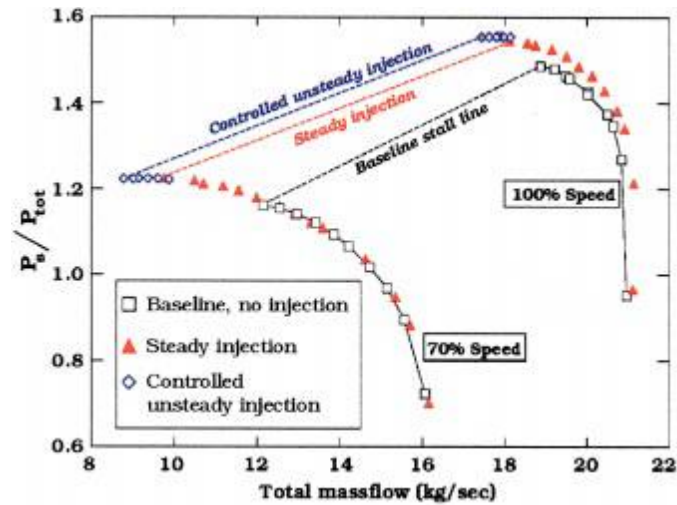
Figure 2: Baseline and injection curve comparison (Suder et al., 2002)

Together with this part, some other important compressor aspects were deepened like the role of tip clearances (Hewkin-Smith, Pullan, Grimshaw, Greitzer, & Spakovszky, 2019)(Khaleghi, Dehkordi, & Tousi, 2016) and the origins and structure of spikes (Pullan, Young, Day, Greitzer, & Spakovszky, 2012).

After having found the best configuration, it was tried to give a reason why that was the best one; unfortunately there weren't conditions sufficient to explain it. The biggest problem involved the injectors exit velocity that was unknown; anyway, an attempt to evaluate it was done and a relationship find in (Liu et al., 2019) was used to try to evaluate the range extension and the relative blade incidence angle using what is reported in (Khaleghi, Teixeira, Tousi, & Boroomand, 2008) but without any success; as (Suder et al., 2002) reported when air is injected, the overal massflow redistributes along the blade span making it a *3D* problem.

1.2 AIM OF THE STUDY

This project thesis work is the last part of a PhD thesis work made by a french student, and it stands inside a big research project called *NumERICCS* which stands for Numerical and Experimental Research for Improved Control of Compressor Surge; it is part of french *ANR – Agence Nationale de la Recherche* and involves french universities like *ENSAM* (Lille), *École Centrale* (Lille), *UPMC – Université Pierre et Marie Curie* (Paris), the french aerospace research organization *ONERA*, and of the french aircraft-engine manufacturer *SNECMA*.

This project involves many researchers and PhD students in studying different aspects of rotating stall. Particularly, this thesis work was a study concerning active flow control for axial compressor rotating stall; control was carried out by an injection system made by air injectors which blow high pressure air in the tip zone of compressor's blades. The main objective of this work were essentially *2*:

- The first one was about test different injection angle, with different injection pressure and injectors layout in order to find out the best scheme able to extend the operating range of the compressor in terms of mass flow rate running at its inside and pressure gain obtained;
- Secondly, the aim was to try to give an explanation of why what was found as the best layout is actually the best one; this part was really complex and it was not possible to give an answer to why. Anyway, it was chosen to investigate what's happening inside the compressor stage when the injection system is on and the overall mass flow rate is constantly reduced until reaching rotating stall. Pressure maps and pressure trend were built thanks to several probes, so that some interesting considerations were outlined.

2 TEST BENCH

2.1 COMPRESSOR'S TEST BENCH CHARACTERISTICS

All the tests were performed using the *CME2* (*Compresseur Mono Étagé 2*) inside the *Laboratoire de Mécanique des Fluides de Lille – Kampé de Fériet*.

Table 1: Compressor's main parameters

Main parameters	Symbol	Unit	Values
Design rotational speed	Ω	[rpm]	3200
Tip diameter	D	[mm]	550
Tip clearance		[mm]	0.5
Hub diameter	d	[mm]	429
Mid span radius	r½	[mm]	244.75
Design speed at the mid span radius	U½	[m/s]	82
Design speed at the tip	U	[m/s]	94
Section		[m^2]	9.3E-02
Rotor blade number			30
Tip chord		[mm]	84
Pitch		[mm]	57.6
Stagger angle		[°]	54
Hub-tip ratio			0.78
Tip clearances-chord ratio			0.6
Tip clearances-span ratio			0.83

Main parameters	Symbol	Unit	Values
Design mass flow rate	q_m	[kg/s]	5.3
Design mass flow speed		[m/s]	46
Design flow coefficient	φ		0.56
Design flow kinetic energy	$\frac{1}{2}\rho U^2$	[Pa]	4120.1
Design pressure rise coefficient	ψ		0.8082
Design pressure ratio			1.065

2.2 TEST BENCH PARTS

2.2.1 Electric motor and transmission system

2.2.1.1 Components

The compressor was switched on by an electric box, which power supplied an electric motor. The electric motor was controlled by the electric frequency and by so the rotational speed was controlled.

Before transmitting the torque to the compressor's rotor, it has been interposed a speed multiplier in order to increment, through a gearbox, the compressor rotational velocity (Figure 3). This device was able to increment the rotational speed by a proportional factor *k=2.345*. So, if the compressor had to run at *3200 [rpm]*, the electric motor had to turn at approximately *22.74 [Hz]*.

The whole system is cooled down by a water circuit that flows inside the gearbox; the circuit is maintained at a pressure of almost 2 bar and the water is coming directly from the aqueduct.

Figure 3: Electric box (1), electric motor (2), speed multiplier (3) and universal joint (4).

2.2.1.2 Switch on, switch off and control

The compressor power on, shutdown and rotational frequency were controlled by a *STROMBERG* control box (Figure 4).

To light up the compressor the procedure was the following: firstly, turn on the electric box and the water cooling system (Figure 3); together with these operations, it is also necessary to power on the compressor oil lubricant system. After that, the valve, numbered as 1, has to be turned to light up the control box display and secondly the black button, number 2, has to be pushed; once it has been pushed, it's possible to hear a thud. Then, the "loc-rem" button, numbered as 3, has to be pushed and finally the green start button, number 4, can be pushed.

At the end the compressor is able to start running by pushing the "minus" button (number 5). The reason why the minus button has to be pushed is that between the electric motor and the universal joint, there was the speed multiplier; this device increases the rotational speed but also changes the turning direction from clockwise to counter clockwise and vice versa. So, looking at the universal joint from the electric box

position, it has to run in a clockwise direction, that is, in this case, a positive direction; this means that the electric motor has to turn in a counter clockwise direction, that is a negative one.

To shut down the compressor, the rotational frequency is reduced through the "plus" button, labelled as 6, and finally, when a rotational frequency lower than *5 hz* is reached, we can push the red stop button, number 7.

In case of emergency there was the red big button, labelled as 8, which enables to turn off the compressor instantaneously.
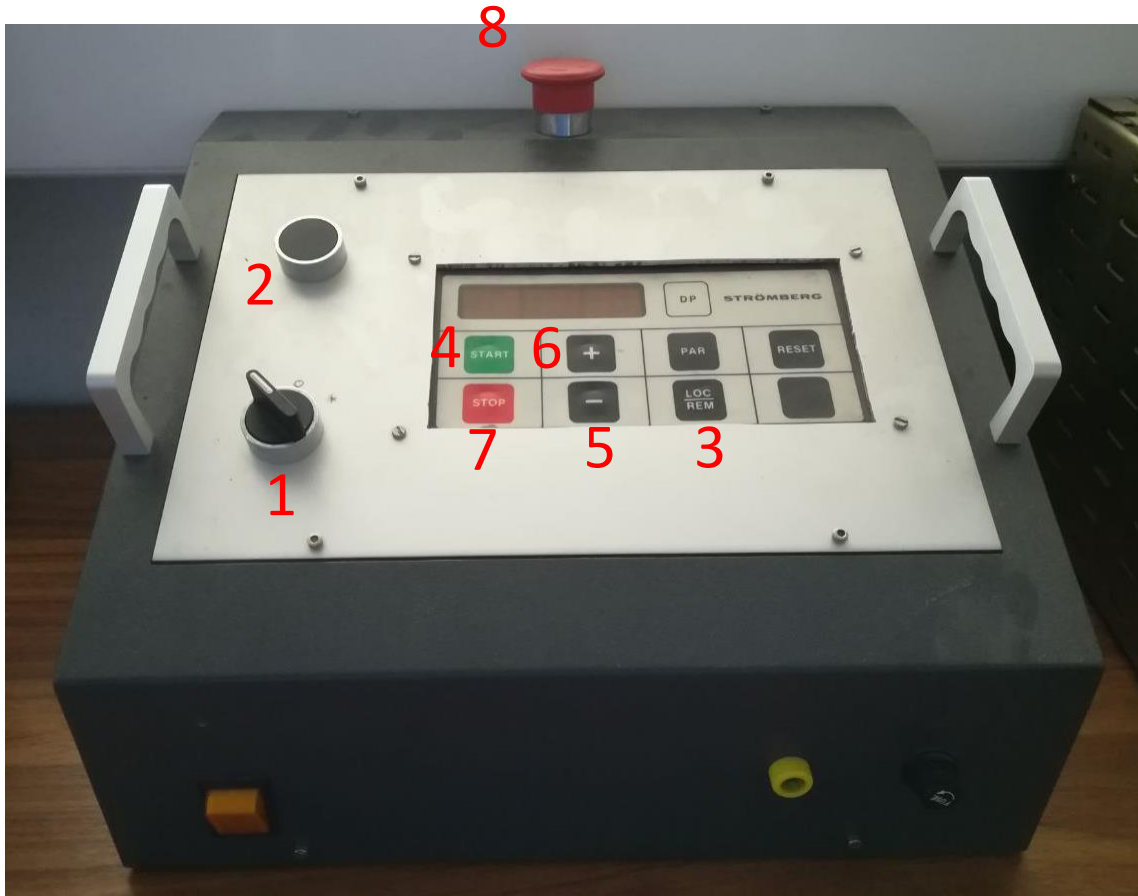
Figure 4: Switch on-off and rotational frequency control box

2.2.2   Compressor body

2.2.2.1   Components

The main body of the compressor is composed by (Figure 5): a filter, placed at the entrance of the air flux; then there's a plenum chamber where the air pass through and the total pressure (through a Pitot tube)

and the temperature are detected. After that, there is a convergent section (in black) in which the static pressure is detected, where the flux is conveyed towards the compressor's blade; finally there is the compressor stage and then the exit section were the air flow is diverted towards the radial direction.

It's important to notice that passing from the convergent section towards the compressor stage, air flux meets the compressor's hub which reduces the main section, causing a speed increasing in the main flow.
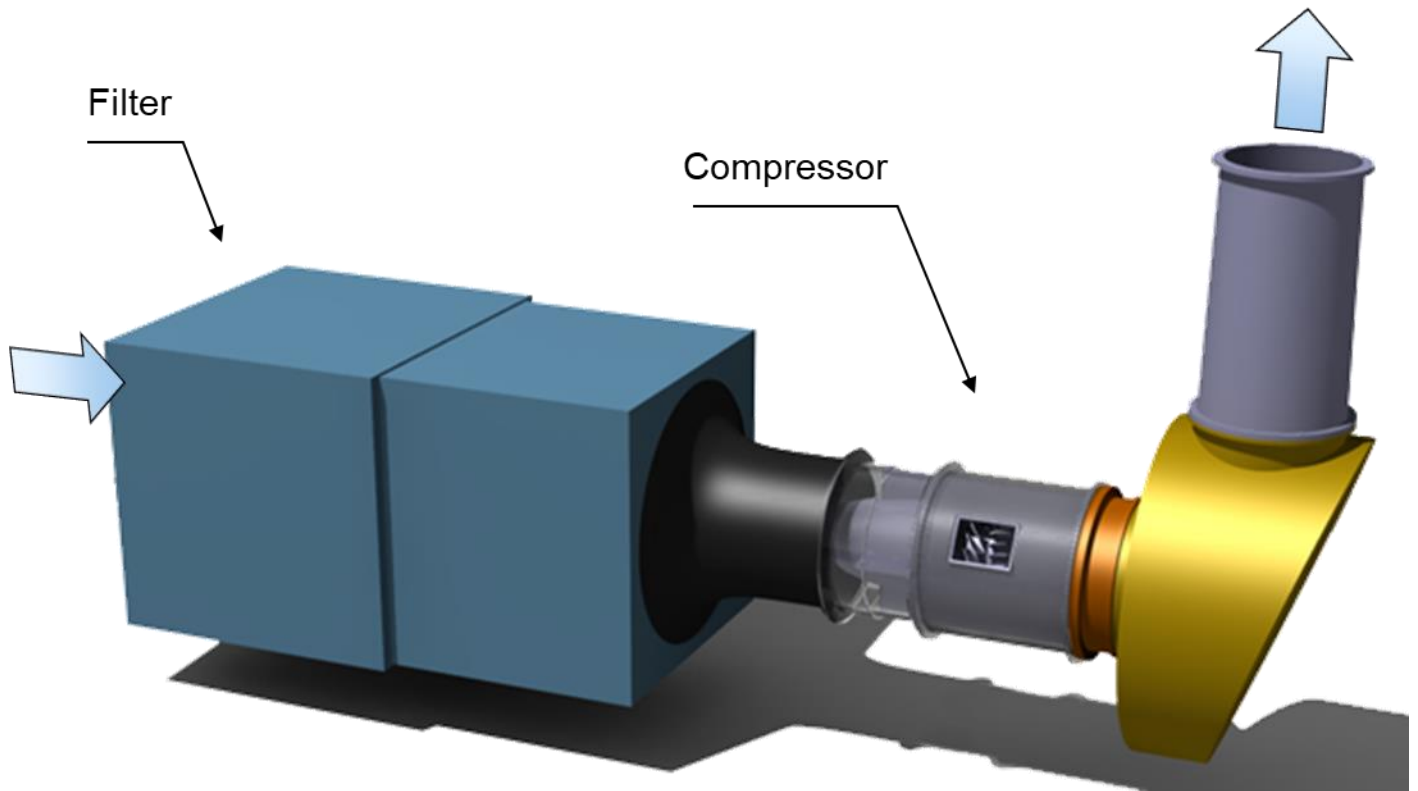
Figure 5: Compressor body's CATIA model

2.2.2.2 Compressor stage

The compressor is made by 30 rotor blades and 40 stator blades. At the tip the incidence angle is about 65°; the maximum rotational speed is *6000 rpm*. The whole compressor is lubricated by an oil circuit; an external pump provides its circulation.
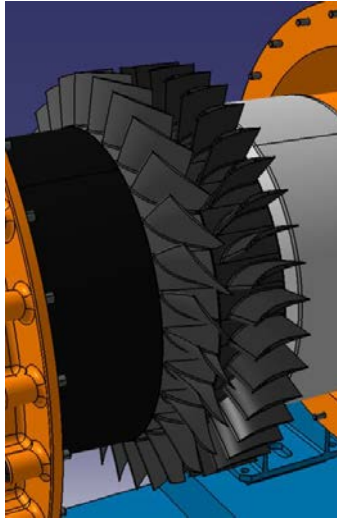
Figure 6: Rotor and stator compressor's CATIA model

2.2.2.3 Regulation

The mass flow is regulated by a throttle valve placed after the compressor stage. Looking at Figure 7, the air flowing inside the compressor is controlled by an actuator (left figure); through this, the throttle valve can be open (using the button labelled *ouvrir*) or close (using the button labelled *fermer*).

By pushing these two buttons, an electric motor is activated (right figure, on top) which makes a chain turn, which enables some toothed wheels to turn and so the exit section is increased or decreased.

For more, there's also the possibility to change the opening and closing valve speed. By means of an adjustment knob (on the left figure) the opening and the closing velocity is controlled; this allows to be more flexible, quicker and either more precise, during all the several parts of experiments.

Figure 7: Control flow box and throttle valve

2.2.3 Active control system

2.2.3.1 Injection system

The active control system consists of a blowing process where air is supplied by an external compressor, stored in a pressure tank and then shot inside the compressor, just in front of the compressor rotor, at a distance of almost *10 mm*.

Figure 8: External compressor and storage tank

The air compression is provided by a screw *KAESER* compressor, *model SM 13T*, which has the following characteristics:

- Nominal power: *7.5 kW*;
- Rotational speed: *2965 rpm*;
- Maximum pressure service: *15 bar*;

Coupled with this screw compressor, there's a pressure tank, model *OKS Otto Klein GmbH D-57223 Kreuztal*, where compressed air can be stored at maximum pressure of *16 bar*; until the compressor is able to guarantee a pressure *15 bar*, tank has *1 bar* safety margin. This reservoir directly feeds the injection system

and is automatically refilled by the screw compressor once the pressure inside tank starts to decrease; its capacity is *500 L*. The compressor has also a humidity separation scheme to purify air.

Air coming out from the tank is controlled by a pressure valve (labelled as A in Figure 9); in order to protect the injection system from breakage, the maximum pressure allowed is *8 bar*. To open or close it, it's sufficient to turn clockwise or counter clockwise respectively, the black knob placed on the top of it. After that, there's a flowmeter that displays the mass flow in terms of *L/min*. Below it, there's a pressure meter that measure atmospheric pressure and humidity.
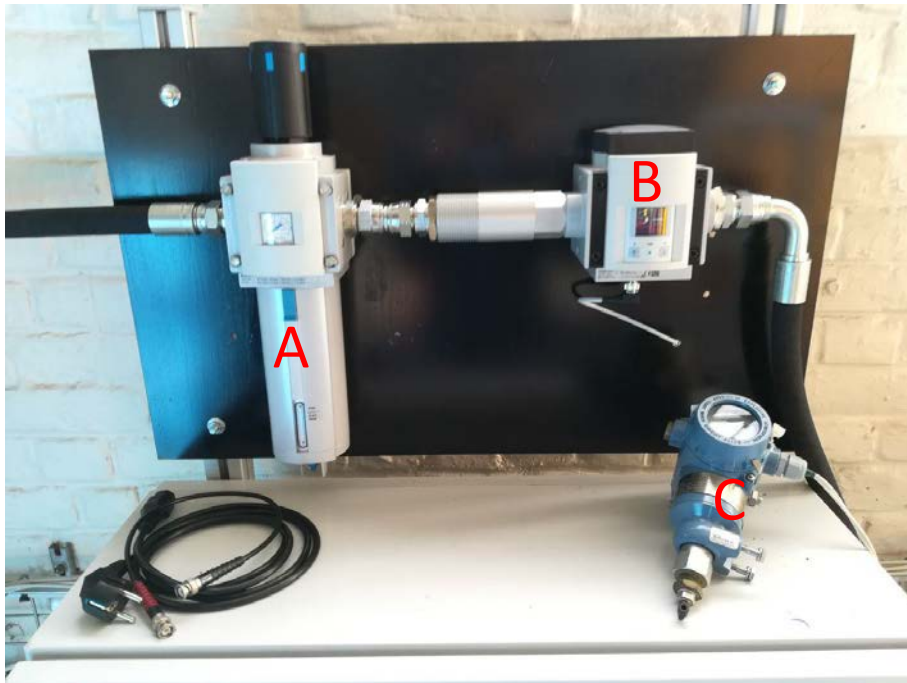
Figure 9: Pressure valve, flowmeter and atmospheric pressure meter

Air injection system consists of the main tube coming out from the flowmeter that splits into two red tubes where the air flows inside. Each of these two red tubes feed a grey vessel where the pressure is measured before mass flow air goes inside the compressor.

These small tanks feed, through four red tube each, an annular tube, where all compressed air is mixed inside, and distributed towards the injectors; from the annular red tube, eight exits come from it, and each of them splits into four small blue tube. Every blue tube leads to the injector devices (as described in Figure 10).
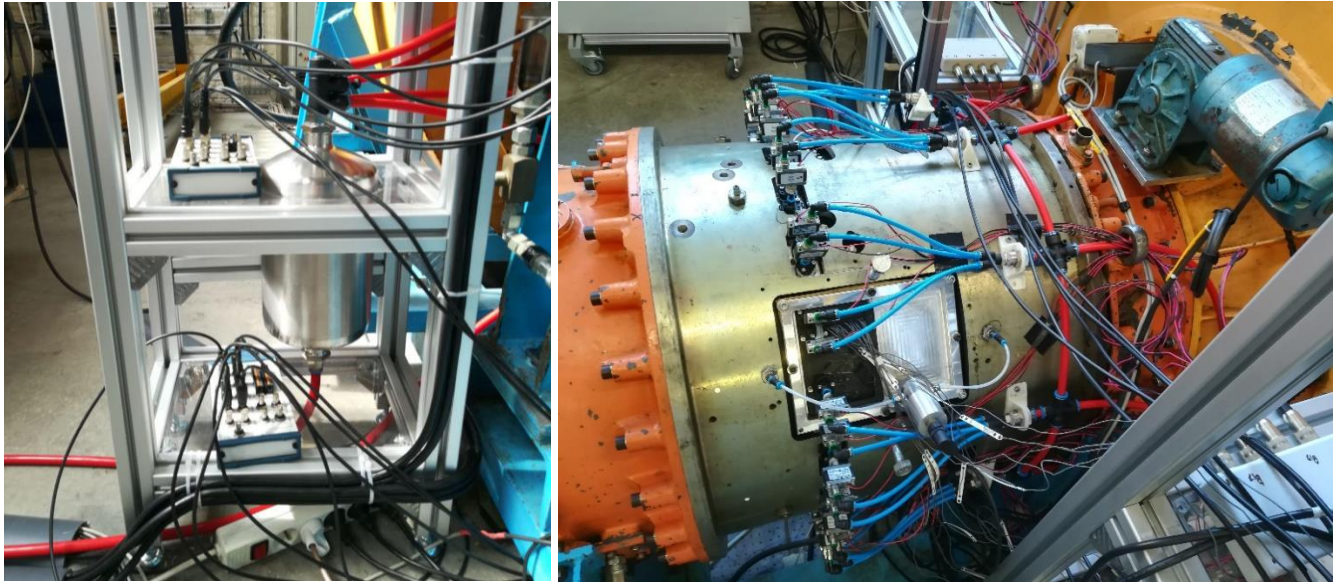
Figure 10: Injection systems

2.2.3.2 Injectors

40 Injectors are placed circumferentially around the compressor's casing; these, are placed paired two by two, as the scheme in Figure 11 shows. Each pair has an angular distance of *5°* while there are *13°* from two consecutive injector pair.
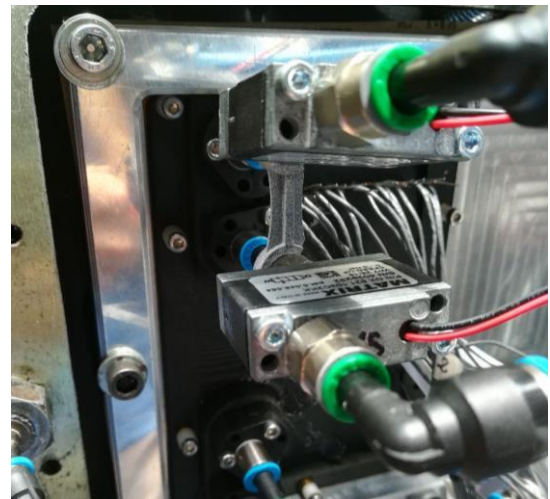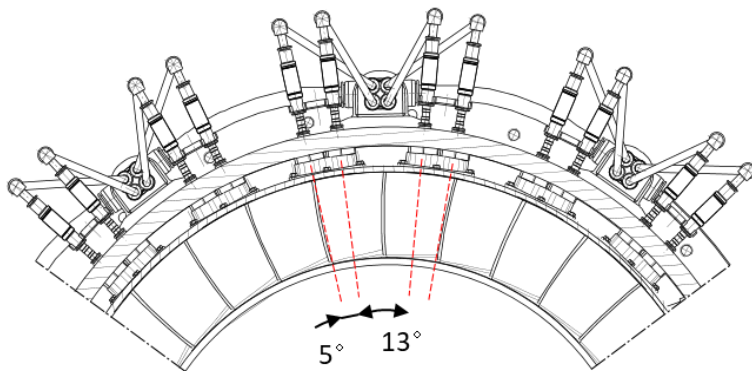
Figure 11: Injectors

Air coming from the annular red ring, flows through the small, light blue pipe towards the injectors. Before entering in the compressor, air is deflected and forced to change its direction of *90°*, so that air enters in an orthogonal direction.

Just before entering the compressor, and after it has been deflected by *90 °*, air pass through a rectangular box where, at its inside, there's a valve which controls both the *open/close* and either the *duty cycle*; particularly, *duty cycle* is a number between *0* and *1* through which is possible to create pulsed injection.

By means of the control system is possible to change the injection frequency, starting from *0* (which means no injection); so it means that we can control and change how many times, during one second, the injection system is blowing. For more, duty cycle gives us the possibility to establish how long air is blowing for each time the injection system is blowing; *duty cycle* equal to *0* means no blowing, independently from the blowing frequency, while *duty cycle* equal to 1 means continuous blowing. For instance, *duty cycle* equal to *0.5* for an injection frequency of *20*, means that there are *20* injections during one second, and during each of these injections, air is blowing for the first half of the injection time, and no blowing in the second half.

Practically, duty cycle is a time step, where its value figures out the time fraction that the injection system is running, and the rest (that is *1-duty cycle*) is the time where it's off; so, *duty cycle* allows the complete opening or closing of the valve. *Duty cycle* equal to *1* means that the system is fully working, independently from the injection frequency.
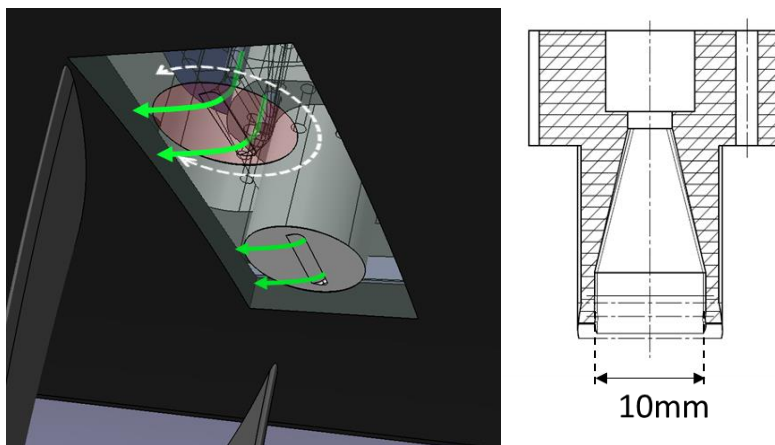
Figure 12: Injectors exit

The exit section of the injection system consists of two parts: a divergent zone firstly, and a deflection one secondly (Figure 12).

The divergent zone is an area where the pipeline's shape is changed, passing from a circular tube to a rectangular section with *10 mm* width and *0.5 mm* height; the exit section is thus *5 mm^2*. Anyway, this type

of shape has shown that the divergent angle is too high, so that air is not able to stay attached at the wall and is coming out with a reduced section of *8 mm* as shown in Figure 13.

The deflection zone consists of a system where the air flux is deflected once more by almost *90°*; practically, air flux, at the end, has an opposite direction of that one passing in the light blue pipeline. Actually, the divergence is of about *86°*, so air flux would not be able to attach at the compressor's casing; anyway, until the jet stream has high velocity, what is possible to see (Figure 13), is that air flux really attaches to the casing due to Coanda effect.
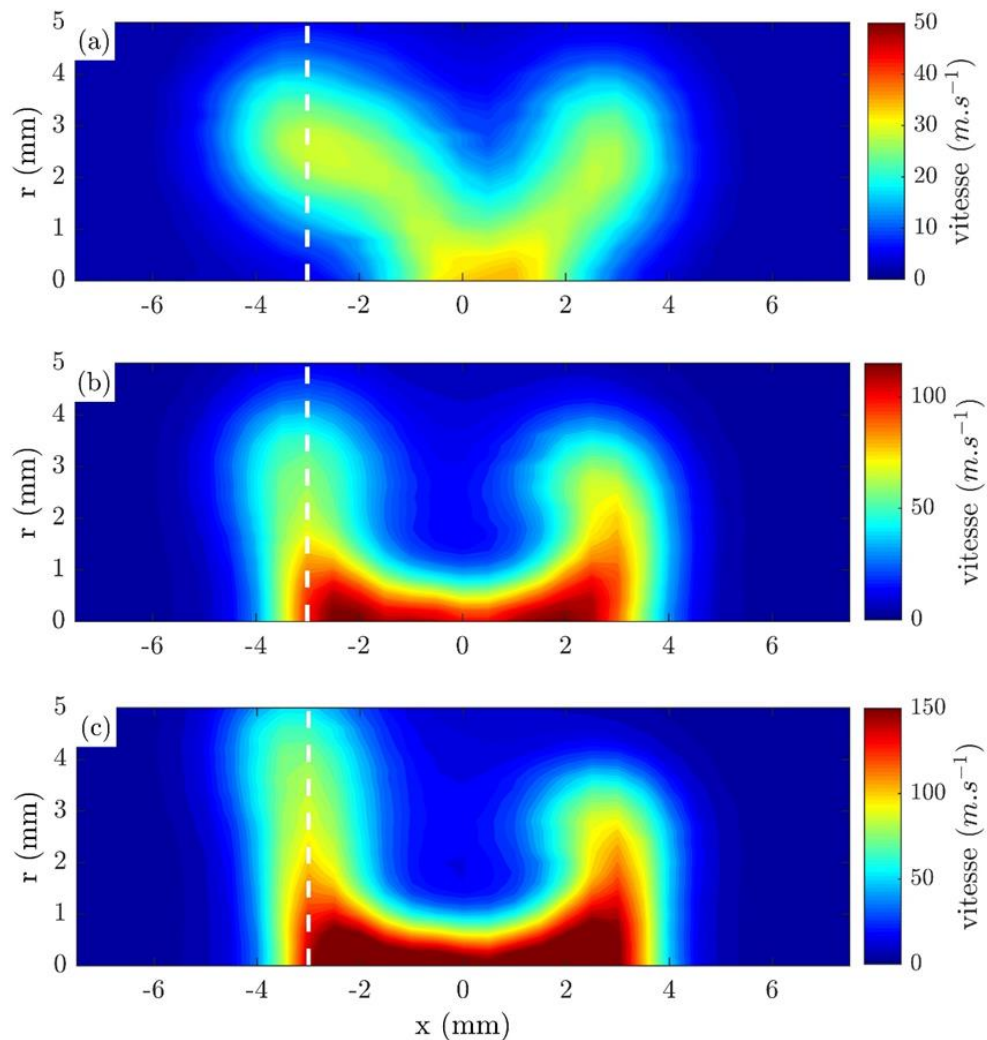
Figure 13: Injector hot wire analysis made by ONERA, with three different mass flow: 20 Lmin⁻¹, 60 Lmin⁻¹, 100 Lmin⁻¹. In the x-axes is shown the width, in the y-axes the height

Injectors are placed just in front of the compressor stage, at a distance of *10 mm*. Another important aspect is that these injectors can be rotate and placed in different position; starting from an axial position (which means that the air stream injected is perfectly in the compressor's axial direction), injectors can be rotated by step of *15°* (white dashed line in left Figure 12). This allows us to change the injector configuration and so, verify if there's one solution that is the best, which is the aim of this work.
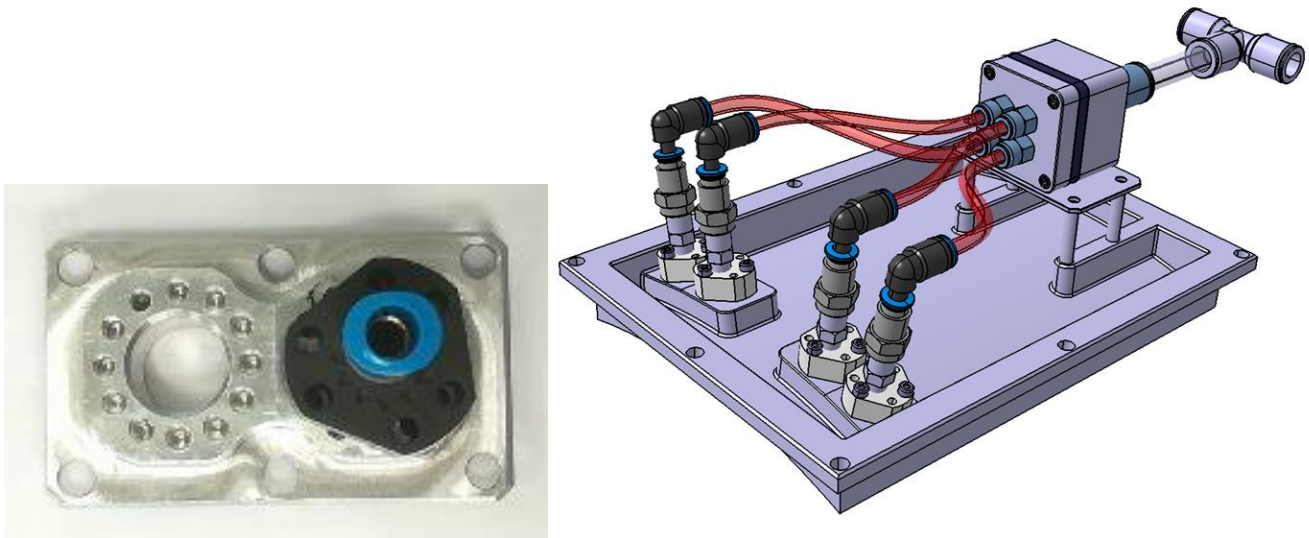
Figure 14: Injectors details and holes for position changing

2.2.4   Pressure probes

To evaluate the behaviour of air stream passing through the blade pitch, with and without the air injection supply, *14* pressure probes were placed outside the compressor, in the casing, just above the blade rotation passage; the first one is placed just *2 mm* before each blade leading edge passage, while the last one is situated only *1 mm* behind each blade trailing edge passage, as described in Figure 15; each of these is equally spaced between the previous and the following one, by *4 mm* distance.
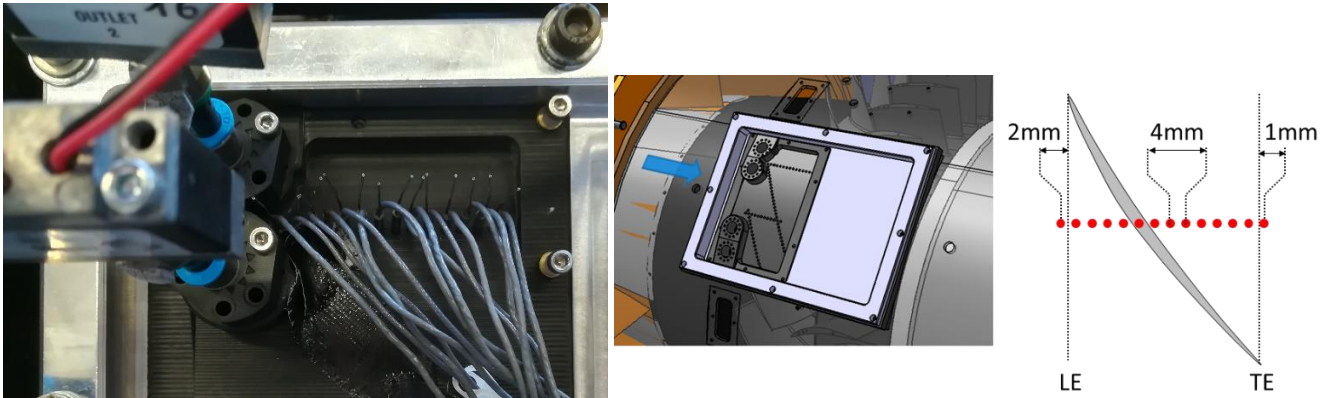
Figure 15: Pressure probes

Each pressure probe is linked with a piezo resistive pressure transducer (see Figure 20); this converts the pressure signal to an analogic one, and send it to the signal amplifier, that is enable to amplify the incoming signal by a specified constant factor that is pre-set.

3 ACQUISITION SYSTEM

3.1 MATLAB ACQUISITION – FIRST PART

Figure 16 presents the left part of the Matlab program interface that has been used to acquire data during the tests. The program has been developed by PhD student Gabriel and is done with the Matlab GUI interface.
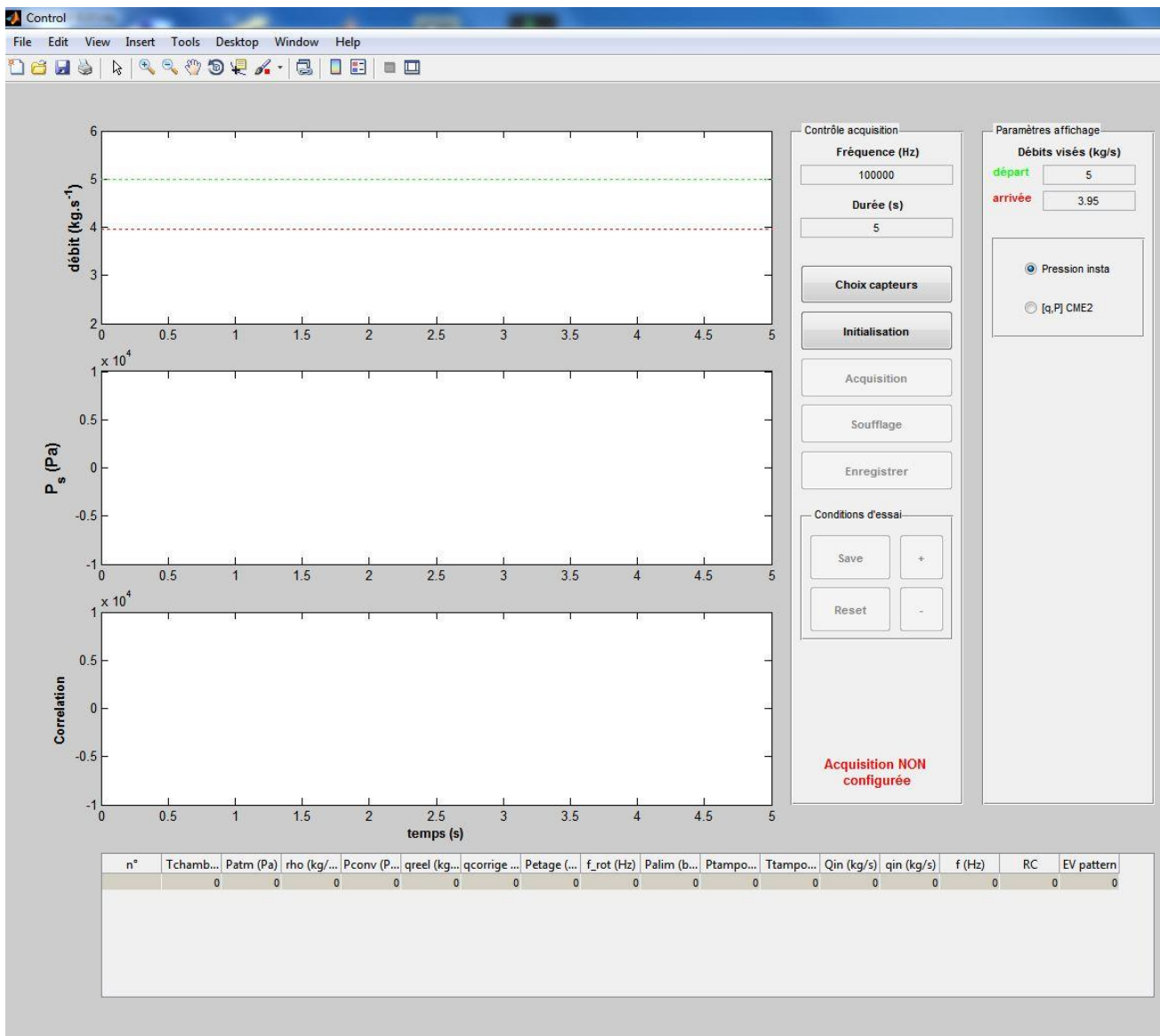
Figure 16: Left part of acquisition system

On the top left of the screenshot Figure 16, is possible to see all the Matlab instruments commonly seen in the programme. The three plots placed in the middle left show, with respect to time, respectively the angle position of a blade taken as a reference (despite in the first y-axes the label is *debit* which stands for flow), the static pressure gained and a particular correlation (that has not been used in the whole work, so it won't be said nothing more about it). Between these three, the most important graph is the second one because shows clearly the pressure trend.

On the middle column of Figure 16 it's possible to find two rectangular boxes: the first one, labelled as *Contrôle acquisition* (acquisition control) and the second one labelled as *Conditions d'essai* (test condition). In the first one, it is possible to find the acquisition frequency, *Fréquence (Hz)* that has been set always at 10000 Hz and the time period for the acquisition, *Durée (s)*. Then there are five buttons: *Choix capteurs* is for type of acquisition to use (it has been used always the same during all tests); *Initialisation* is the initialization of the acquisition system; *Acquisition* is the button that allows to acquire the pressure trend during a period of time as set in *Durée (s)*; *Soufflage* is the button through which is possible to turn on the whole injection system; finally, with *Enregistrer*, it's possible to save the pressure data acquired by the *Acquisition* button.

On the box below, labelled as *Conditions d'essai (test conditions)*, it's possible to find four buttons: *+*, *-*, *Save* and *Reset*. These four buttons allow, respectively, to add a line or erase one in the bottom table in Figure 16, and to save or reset the table created with the previous two buttons.

The column on the right side of Figure 16, labelled as *Paramètre affichage* (parameter display), allows to display two straight lines in the first of the three graphs, through the command *Débits visés* (flows display); in the same column it's possible to find two options: *pression insta* and *[q,p] CME2*. The first option allows to pick the instantaneous pressure value while the second one evaluates the mean pressure value in a time interval of *1 s*. The instantaneous pressure option has been chosen when the pressure trend had to be drawn, while the mean value was chosen when it was necessary to build the compressor characteristic curve. Anyway, the instantaneous pressure was always selected.

The bottom table stands for acquiring a specific point during the compressor running. To do so, it's necessary to push the *+* button available in the *Condition d'essai* box; once it has been done, a line will appear in the box. To delete the last data-line acquired, it's necessary to push the – button. In this table there are many columns, corresponding to several data; starting from left to right there are:

- *n°*: number of data-line acquired;

- *T chambre*: temperature inside the *chambre de tranquilisation*, before the convergent section expressed in *°C* (see Figure 5);

- *P atm*: atmospheric pressure in *Pa* (see Figure 9, C);

- *rho*: atmospheric density in *kg/m³* evaluated as:

$$\rho = \frac{P}{R \cdot T}$$

where *R* is the universal specific gas constant equal to *287.05 J/(kg*K)*, *P* is the atmospheric pressure in *Pa* and *T*, the atmospheric temperature in *K*.

- *P conv*: pressure inside the convergent section in *Pa* (see Figure 5);

- *q reel*: real mass flow rate inside the compressor, expressed in *kg/s*;

- *q corrigé*: compressor's mass flow rate corrected at *0°C*, in *kg/s;*

- *P etage*: compressor stage gain, in *Pa*;

- *f_rot*: electric motor frequency, in *Hz*;

- *P alim*: air pressure measured in the pressure valve in *bar* (see Figure 9, A);

- *P tampon*: air pressure measured in the small vessel, in *bar* (see Figure 10, left);

- *Q in*: overall injectors mass flow rate in *NL/min*;

- *q in*: injector mass flow rate in *NL/min* (this value is always incorrect);

- *f*: injection frequency in *Hz*;

- *RC*: duty cycle;

- *EV pattern*: a vector that has 20 components, each for the paired injectors; each of them could be a *0* or a *1* if the corresponding electrovalve, and so the two injectors, is open or close.

In the bottom part of Figure 16, it's possible to see the written in red, *acquisition non configure*, which means that the acquisition system is non configurated. To start the configuration is sufficient to push *choix capteurs* button and select which type of acquisition is needed; once it has been done, it's sufficient to push *initialisation button*. Immediately, a yellow written will appear instead of the red one with the words *acquisition en cours*; it will last for a few seconds and finally a green written will appear with the words *Acquisition prête*. At this point the acquisition system is able to run.

3.2 MATLAB ACQUISITION – SECOND PART

Figure 17 presents the left part of the Matlab program interface that has been used to acquire data during the tests. Here there are two boxes and other two tables; starting from left to right it's possible to find: *infos machine, contrôle electrovannes* and the tables.

The two tables on the right side of Figure 17, contain *14* lines, each corresponding to the pressure probe used to obtain the pressure maps.

Figure 17: Right part of acquisition system

3.2.1 "Infos machine"

The *infos machine* box is splitted into four part; in the first part it's possible to find the atmospheric pressure in *Pa*, the air temperature flowing into the compressor in *°C*, and then the air density flowing inside the compressor, in *kg/m³*. Temperature and air density are automatically given respectively by temperature

sensor and calculation using knowing parameters and some correlations, while atmospheric pressure is inserted manually once the atmospheric pressure meter is read (see Figure 9, B).

In the second part is possible to read the mass flow rate and corrected mass flow rate instantaneous values (*dèbit réel* and *dèbit corrigè*), both expressed in *kg/s*, flowing inside compressor. The third value has never been used, and, the author doesn't know at what it refers to.

In the third one there are several parameters dealing with the injection system; here, it's possible to find the feeding pressure (*pression alim*) in *bar*, the feeding temperature (*tempèrature alim*) in *°C*, the total mass flow rate (*dèbit total*) inside the whole injection system, expressed in *kg/s*, the single injection mass flow rate (*dèbit unitaire*), in *kg/s*, and the injection velocity (*vitesse d'injection*) in *m/s*, evaluated trough an isoentropic relation; anyway, it will be shown that this type of relation will be far from the real values of injection velocity.

Then, on the last part, there are four parameters concerning the electric motor; firstly, it's possible to find the standard rotational speed (*vitesse de rotation standard visée*) in *RPM*, then the real rotational speed (*vitesse de rotation rèelle visée*) in *RPM*, thirdly, the electric motor frequency (*f moteur visée*) in *Hz*, and finally the rotational speed (*vitesse de rotation*) in *RPM*.

Standard rotational speed refers to the average rotational speed at which the compressor should run; this value is filled in by hands, and once it's done, automatically the electric motor frequency changes and suggest which is the frequency at which the electric motor has to run. So, if the electric motor frequency is changed towards values very close to that one displayed in *f moteur visée*, the compressor would run at a rotational speed that is very close to the standard rotational one.

3.2.2 "contrôle soufflage"

The *contrôle soufflage* box allows to play, in the top part of it, with some parameters concerning the injection system; firstly, it's possible to choose the injectors frequency (*fréquence*) and secondly the duty cycle (*rapport cyclique*). Both these values are applied to the whole injection system, so there won't be injectors playing with different frequency or different duty cycle between different injectors.

In the part below, it's possible to find a particular grid, composed by *20* blocks: each of them represents an electro valve. All of them can be open, so air flows inside injectors, or close. It's possible to decide which blocks are open and which other are closed; to do so, it's necessary to click on each block. By doing so, it changes its

colour; red, means that the block, and so the electro valve, is off, otherwise, if the colour block is green, the electro valve is on. This means that it's possible to create an infinite combinations of injector configurations.

It's important to say that the block labelled as *Block1* is that one placed in the top part of the compressor's casing. As an example, in Figure 18 is possible to see two different injectors blowing configuration: on the left, all injectors are on (*20* electro valves that is *40* injectors), while on the right half injectors are on (*10* electro valves that corresponds to 20 injectors). Notice that each electro valve controls a pair of injectors; this means that the second configuration has pair of injectors working and pair of them not, alternatively.
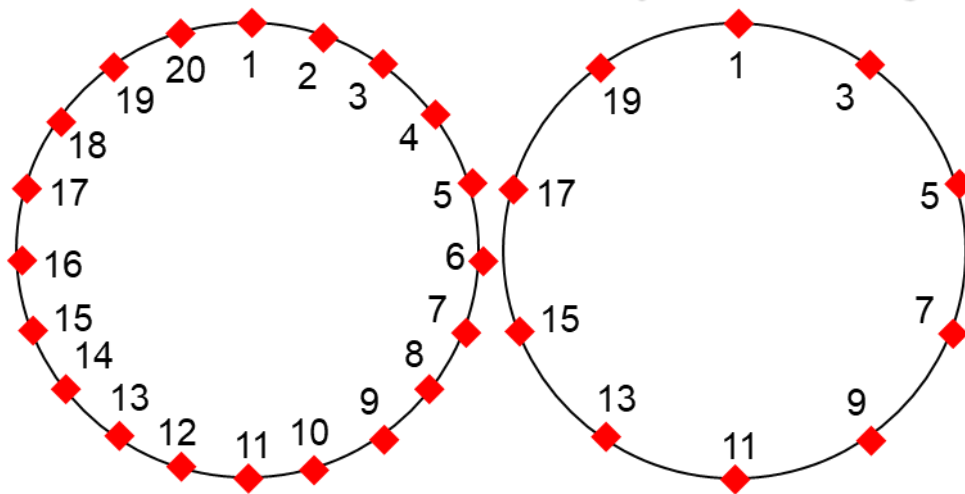
Figure 18: Two different injection configuration

Below the electro valve scheme, there are two different buttons: *ALL* allows to activate all electro valves (all the *20* blocks become green), while *NONE* deactivate all the electro valves (every block becomes red).

3.3 ACQUISITION DEVICES

Figure 19: Data collecting and computer

To collect, display and store data, there was a signal collector (left on Figure 19), a powerful computer from National Instruments and a hard disk where store data. The signal coming from the Matlab program are distributed to signal collector which provides to send it to the electro valves.

To convert pressure signal coming from the pressure probes into an electric analogic one, a piezo resistive pressure transducer is used; then, to amplify it, a signal amplifier is placed. Sometimes the signal amplification had to be reduced because the signal was too strong.

Figure 20: Signal amplifier and piezoresistive pressure transducer

4 EXPERIMENTAL SETUP

The first period was all about doing some tests, they were done specifically for the last of PhD student's Gabriel work. So, several different injection configurations were tested; different injection frequencies were used and, also, different duty cycle. After one month and a half, approximately, the time was ready to start the test campaign.

4.1 FIRST PART: BEST CONFIGURATION ANGLE

4.1.1 Introduction

The first part of this thesis work involves tests in order to find the best injection angle configuration. To do so, some parameters were fixed in order to evaluate the effect of some of them. It was set:

- Duty cycle equal to *1*; this means that, independently from injectors frequency, injection will always be continuous;
- Fixed rotational speed equal to *3200 RPM*; this means that, the electric motor frequency should be fixed. Anyway, due to environmental conditions, frequency tends to change a little bit; if the weather is cold, it tends to decrease, otherwise, if it's warm, or even hot, it tends to increase;

Before each test, the atmospheric pressure was taken, and set in the acquisition Matlab program system; in the same way, the duty cycle was set as *1*, while care must be taken with rotor frequency because, due to the warm up of the entire compressor system, it tends to increase, as described above. It was also essential to avoid long period duration tests, because the lubricant system is made by oil; this one, once it starts to circulate in pressure inside the compressor, it tends to warm up and so decrease its viscosity and this means it expands a little bit. Usually this is not a problem, but in long time series of tests, this would be a problem because circulation pump will not be able to pump back all the oil to the main reservoir, and this will start to accumulate on the small one, until it won't be able to contain any other oil and it will fall out of it, causing a leakage.

Taking into account all these things, tests were carried out playing on the following three important parameters:

- *Injection angle*;

- *Injection pressure;*
- *Injector number.*

4.1.1.1 Injection angle

In order to evaluate if there were an optimal angle configuration at which the compressor was able to reach the minimum mass flow rate, and so, work with the lowest value of it without reaching stall conditions, several injection angles were tested.

Notice that, to clarify, injection angles were considered negative when the tangential component of injection velocity (that is the component in the same way of compressor tangential rotational speed) is on the opposite direction with respect to the tip rotor velocity direction, while injection angles were considered positive when they were in the same direction.
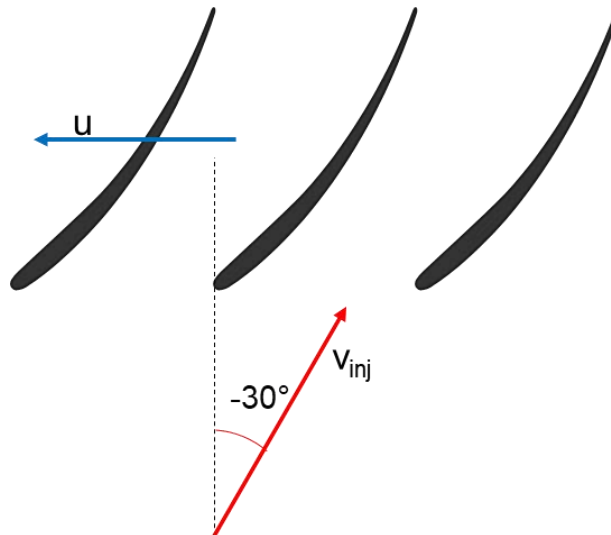
Figure 21: Injection angle and blade rotating scheme

Until the injection angle positions are forced to be of step of 15°, the injection angle configurations tested were:

- *+15°*
- *0°*
- *-15°*
- *-30°*
- *-45°*

4.1.1.2   Injection pressure

Different injection pressures were performed, to understand which was the relation, if there were one, between injection angle and pressure; until maximum injection pressure allowed by the whole blowing system was of 8 bar, the injection pressure configurations tested were the following:

- *1 bar*;
- *2.5 bar*;
- *4 bar*;
- *5.5 bar*;
- *7 bar*

4.1.1.3   Injectors number

Another parameter that has been investigated, was injectors number. It has been tried to verify if there is a kind of relationship between injectors number and angle. Until injectors were paired controlled, each with an electro-valve, here it is reported the number of injectors coupled blocks, turned on during tests:

- *5 blocks*;
- *8 blocks*;
- *10 blocks*;
- *11 blocks*;
- *14 blocks*;
- *17 blocks*;
- *20 blocks.*

For every configuration it had been tried to be axial symmetric with respect to the rotation centre.

To deal with these three types of parameters, it had been keeping fixed two of them, changing the third one.

4.1.2   Test procedure

The most cost affecting operation was changing the injection angle; it's a long operation taking more than an hour changing one by one, each injector position; this was particularly uncomfortable in some particular

zones, not easily accessible. So, every test session was performed using a fixed injection angle configuration, while the other two parameters were changed throughout the whole session.

As things were so, each test session was split into two parts: the first one, where different injection pressures were tested while all *40* injectors were blowing, and the second one where different injectors configuration were performed and injection pressure remained constant. In each session anyway, a compressor curve without any type of control (the so called *no control case*) is recorded.

First step to do for each test is to light up the compressor; the procedure is described in paragraph 2.2.1.2, and, during the power on and carrying out the tests, the lubricant oil level has to be controlled. After that, atmospheric pressure had to be detected by means of the pressure meter (see Figure 9) and report to the special space in the Matlab GUI interface (see 3.2.1).

Once it has been done, it's necessary to set the injection pressure; to do so, it's necessary to play with the pressure valve (see Figure 9) to be as close as possible to the target value, and then check if the value is close enough by means of the *pression alim* (see 3.2.1). it has been chosen a tolerance of *0.1 bar*, but it was possible to reach only a range of *0.3-0.5 bar*. This means that, if the target value was *3 bar*, acceptable values for the author, were included, at best, within *2.7 bar* and *3.3 bar*. It's important to say that pressure valve is very sensible at lower pressure (from *0 bar* up to *2 bar*); a small movement of it changes rapidly the pressure. It's always sensible when it turns to open up the circuit while it isn't when it's necessary to close it a little bit; so the best way to set the pressure is to approach the target value from a lower one and tried to reach the desired, turning the valve slowly; if the pressure is too high, it's necessary to close the valve of a great amount and then try to approach the target value from below, as described in the previous lines. This was also one of the most time spending situation during the tests. Obviously, all these types of operations were done while compressor was running, so a pair of work caps are absolutely needed.

After that, the real acquisition procedure starts; it has been decided, for this first part of tests, to start at a corrected mass flow rate of *4.8 kg/s*. To target this value, the control flow box (see Figure 7) had been used; by means of the opening and closing buttons and of the adjustment knob, the desired mass flow rate was reached.

So, the *4.8 kg/s* mass flow rate was the first point detected in all these tests sessions. To record the values at this point, it is sufficient to push the *+* button as described in the last part of part 3.1. Once it had been done, the mass flow rate is reduced by a quantity of almost *0.2 kg/s* and another value is recorded. This step

quantity is used just to arrive at *4.4 kg/s* where the mass flow rate step is reduced; so, next mass flow rate was *4.3 kg/s* before it had been reduced again in order to reach a mass flow rate of *4.25 kg/s*. Obviously, to be so precise is necessary to play with the adjustment knob; usually passing from *4.8 kg/s* up to *4.3 kg/s* mass flow rate, the author had used a *30%* of the closing speed, while, for lower values, approaching rotating stall, he had chosen almost a *20%* of it.

If it had been recording the *no control case*, once arrived at *4.25 kg/s* mass flow rate, it's necessary to close slowly the closing valve while recording freely some points, so that they are fairly thick in the area near the rotating stall; otherwise, at this point, the injection system has to be turned on and left it on while recording some data points and at the same time reducing the mass flow rate.

If it had been recording the control case, it was necessary to activate the injection system; so, firstly the mass flow rate was brought at each target value, as described above and then the *soufflage* button was turned on. It was necessary to wait few seconds before record the data point with the blowing on, usually *3-5 s*. After having recorded the point, the blowing system was shut down because, especially at the high pressure, the pressure tank empties very quickly. Once at *4.25 kg/s* the blowing system has to be left on to measure the real effectiveness of the active control system; indeed, mass flow rate will be much lower than that one reached without the injection system, and so, if there isn't the possibility to turn on, record data and then turn it off again.

During this first part, meanwhile recording data concerning all the *40* injectors and different injection pressures, the *20* injector configurations were also performed and recorded. This was done because the injection configuration was easier and faster to implement than the pressure one.

In the second part, pressure was fixed at *7.5 bar* and the injections configuration was changed. For each test pressure, the procedure was that one as described above: starting from *4.8 kg/s* mass flow rate, data were recorded lighting up and shut down the injection system only for a few seconds, until *4.25 kg/s* where it was left always on.

By the way for each data file, all points recorded were stable, except the last which was taken when compressor was in rotating stall; it was fundamental to be as precise as possible to take the last stable point, and also to avoid taking two different unstable point, otherwise the post processing program would give some output results which are not correct.

In the end, data recorded would be like:

- *1* data file where blowing was off, named, for example, as *0-baseline-0°-3200RPM*;
- *5* data files with blowing and all injectors on, labelled, for example, as *20blocks-1bar-15°-3200RPM-DC1*;
- *5* data files with blowing and half injectors on, labelled, for example, as 1*0blocks-1bar-15°-3200RPM-DC1*;
- *6* data files with blowing and different injectors configurations on, labelled as *7.5bar-08blocks- -15°-3200RPM-DC1*;

So finally, the overall amount of data files for each injection angle configuration is *17*.

4.2 SECOND PART: PRESSURE FIELD

This second part was a study concerning the pressure field of the five different injection angles, in order to see what's happening inside the blade pitch with blowing system on; the compressor rotating speed was kept constant at *3200 RPM* as in the previous case, and the *duty cycle* was always equal to *1*. So, injection angles were the same as the first part, while injection pressures were different from that one tested previously; here it was tested the following pressure, while injection configuration was fixed with *20 blocks* on (*40* injectors on):

- *1 bar*;
- *3 bar*;
- *5 bar*;
- *7 bar*.

In the same way, different injection configurations, with respect to the above ones, were tested while injection pressure was kept constant and fixed at *7 bar*:

- *5 blocks*;
- *10 blocks*;
- *15 blocks*.

In the end, the overall amount of data files would have been the following:

- *1* data file where blowing was off, named, for example, as *baseline- -45°-3200RPM*;

- *4* data files with blowing, all injectors on and different injection pressure, labelled, for example, as *20blocks-7bar-30°-3200RPM*;

- *3* data files with blowing and different injectors configurations on, labelled, for example, as 1*0blocks-7bar-30°-3200RPM*;

4.2.1   Test procedure

Once the acquisition system is initialized, as described in paragraph 3.1, and the compressor is on, everything is ready for acquire the pressure field data. Firstly, it's necessary to check that frequency acquisition (*Frèquence* in Figure 16) is sufficiently high; this value had never been changed and was set at *100000 Hz*. Secondly, it is necessary to set the *insta pressure* option (Figure 16); finally, it needed to take care about the acquisition time period, because it's fundamental to set it in such a way that tests could be done inside the time duration window: usually this value had been set between *15 s* and *20 s*.

As what it had to be analysed was rotating stall, all this kind of tests were performed dynamically, moving from a starting mass flow rate, here set at *5.0 kg/s*, towards rotating stall and while the compressor system evolved towards it, record all pressure data. The adjustment knob (Figure 7), that controls the throttle valve opening and closing, was set at *80%* (when at *100%*, throttle valve reduces or increases mass flow rate of an amount of *0.2-0.3 kg/s*); this means that, without any control system, rotating stall would had been reached in almost *4 s*.

To start the acquisition system is sufficient to push the *acquisition* button; usually, the program has a delay in response time of about *1-2 s* after which the three plots on Figure 16 would start to fill in. In the same way, when the acquisition time is over, the system has another delay in response time after which is possible to save the data pushing the *Enregistrer* button.

If the test involves the *no control case*, the procedure is to place the compressor at *5.0 kg/s* mass flow rate and start the acquisition; after *4-5 s*, close the throttle valve (*Fermer* button on Figure 7) and keep the button pushed until rotating stall is reached; then wait the acquisition time is over, and finally save data.

Otherwise, if test was with injection system on, then repeat the same starting procedure as for the *no control case*; after placing the compressor at *5.0 kg/s*, start the injection pushing *soufflage* button; wait *4-5*

s and then start to close the throttle valve as described above; note that with injection on, compressor will reach later rotating stall as the adjustment knob is set at fixed value.

5 ANALYTICAL METHODS

Three programs were built up for data post processing; each of them was written in Matlab. Two of them were made by PhD student Gabriel, while the other one by the author; here we report the name of them:

- *traitement_soufflage_bis*;
- *Super_programma*;
- *Interface_bis*.

5.1 "TRAITEMENT_SOUFFLAGE_BIS"

Traitement_soufflage_bis was a program built with the Matlab GUI interface; its task is firstly to calculate different parameters and then, to compare these different parameters by means of graphs, as Figure 23 shows.

5.1.1 Calculations

Once program is launched, a small window will open asking which type of interface program is needed. What it had always been used is the performance button (Figure 22), which opens the interface in Figure 23.

Figure 22:"traitement_soufflage_bis" opening window

By pushing the performances button, a directory containing data to process has to be select; after that, the interface, as reported in Figure 23 will appear.

On its left side, there is a list of data files included in the selected directory; next to them, in the small box labelled *Actions* there are several buttons for the computing of graphs; on the central part, two empty charts are displayed and finally the part below contains a long table in which several data are reported.
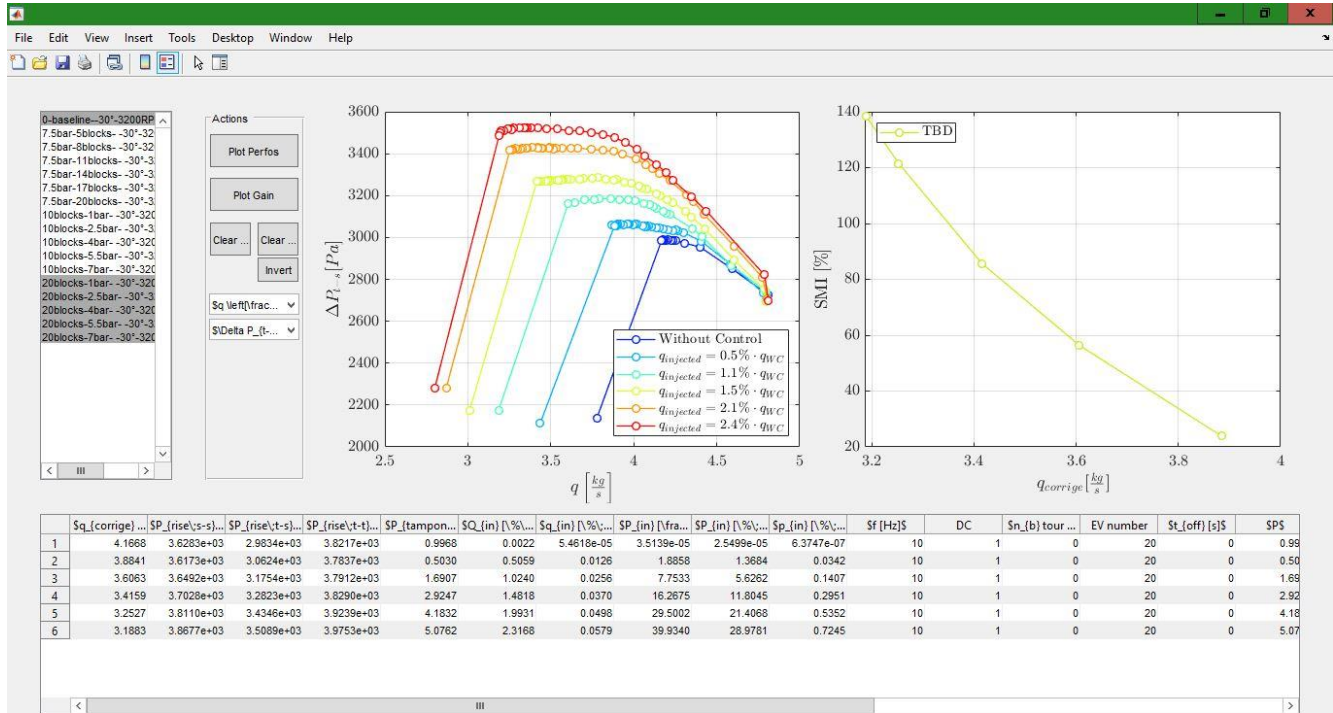
Figure 23: "traitement_soufflage_bis" program

As described in paragraph 3.1, acquisition program record *16* different data parameters; in the program, starting from them, several others are evaluated and reported in the bottom part of program interface. The new ones are presented below, starting from that concerning compressor and then that involving injection system.

5.1.1.1 Parameters concerning compressor

- Inlet axial velocity:

$$V_{x01} = \frac{q_{corrige}}{\rho} \cdot \left(r_{casing}^2 - r_{hub1}^2 \right) \cdot \pi$$

Where r_{casing} is the internal compressor radius, equal to *0.275 m*, and r_{hub1} is the hub radius inside the compressor before rotor blades, equal to *0.204 m*; the whole term on the right of fraction, represents the

flowing area just in front of rotor blades. So, this velocity is that one approaching rotor section, purely axial, and is expressed in *m/s*.

- Outlet axial velocity:

$$V_{x02} = \frac{q_{corrige}}{\rho} \cdot \left(r_{casing}^2 - r_{hub2}^2\right) \cdot \pi$$

As in the previous equation, this is mass flow air velocity flowing inside compressor in section after compressor stage, expressed in *m/s*; r_{hub2} is the hub radius in the section after blades stage.

- Blades mean velocity:

$$U = \frac{v_{rot}}{60} \cdot 2 \cdot \pi \cdot \frac{\left(r_{tip} - r_{base}\right)}{2}$$

v_{rot} is the compressor rotational speed, *3200 RPM*, r_{tip} is the tip blade radius, equal to *0.275 mm*, and r_{base} is the base blade radius, equal to *0.207 mm*; this quantity is expressed in *m/s*.

- Static to static pressure gain:

$$P_{s-s} = P_{etage}$$

Expressed in *Pa*.

- Total to static pressure gain:

$$P_{t-s} = P_{etage} - \frac{1}{2} \cdot \rho \cdot V_{x01}^2$$

Evaluated in *Pa*.

- Total to total pressure gain:

$$P_{t-s} = P_{etage} - \frac{1}{2} \cdot \rho \cdot (V_{x02}^2 - V_{x01}^2)$$

Calculated in *Pa*.

- Static to static pressure coefficient:

$$\Psi_{s-s} = \frac{P_{s-s}}{\frac{1}{2} \cdot \rho \cdot U^2}$$

Which is a dimensionless number.

- Total to static pressure coefficient:

$$\Psi_{t-s} = \frac{P_{t-s}}{\frac{1}{2} \cdot \rho \cdot U^2}$$

- Total to total pressure coefficient:

$$\Psi_{t-t} = \frac{P_{t-t}}{\frac{1}{2} \cdot \rho \cdot U^2}$$

- Flow coefficient:

$$\Phi = \frac{V_{x01}}{U}$$

Which is also dimensionless.

- Stage power:

$$W_{etage} = \frac{P_{t-t} \cdot q_{corrige}}{\rho}$$

Expressed in *Watt (W)*, means the power gained by fluid, passing on the blade stage.

5.1.1.2 Parameters concerning injection

- Injected mass flow:

$$debit\_injecte = \frac{Q_{in_N L}}{60 \cdot 1000} \cdot \frac{p_0}{T_0 \cdot R}$$

Where *60* and *1000* represents the conversion from *min* to *s* and from *L* to *10^3 L*, p_0 is the standard atmospheric pressure, *101325 Pa*, T_0 is the Kelvin temperature at *0°C* and *R* is the universal specific gas constant equal to *287.05 J/(kg*K)*. It represents the unit mass flow of an injector, and is expressed in *kg/s*.

Set the injector exit area as the product between height and width, it results in: *sinj=0.0005*0.01=5*10^6 m²*, then it's possible to compute other parameters:

- Injectors on, overall exit area:

$$Sinj = 2 \cdot Nb_{EV} \cdot sinj$$

Where Nb_{EV} is the number of electro valves that are on and *2* is because each electro valve controls a pair of injectors. It's expressed in *m²*.

- Time off injection during one cycle:

$$t_{off} = \frac{1 - DC}{f}$$

Where *DC* is the *duty cycle* and *f* is the frequency; it's expressed in *s* and represents the time during each cycle in which injectors are not blowing. In tests done, it had been always equal to *0*.

- Rotation off injection during one cycle:

$$Nb_{tour\,off} = \frac{v_{rot}}{60 \cdot f} \cdot (1 - DC)$$

It represents the number of rotations during each cycle in which the injection is off; it's a dimensionless parameter and in all tests done, like previous case, it had always been equal to *0*.

- Overall mass flow injected:

$$Q_{in\_kg} = \frac{Q_{in\_NL}}{60 \cdot 1000} \cdot \frac{p_0}{T_0 \cdot R}$$

Where Q_{in_NL} is overall injected mass flow measured in *NL/min*; this new parameter is evaluated in *kg/s*.

- Single injector mass flow blown:

$$q_{in\_kg} = \frac{Q_{in_{NL}}}{2 \cdot Nb_{EV}}$$

It's the mass flow in *kg/s* injected by every injector that is on.

- Injection velocity:

$$V_{in} = \frac{Q_{in\_kg}}{\rho \cdot Sinj \cdot DC}$$

Expressed in *m/s*; velocity will be widely discussed later.

- Main inlet velocity (without injected mass flow):

$$V_{x1} = \frac{q_{corrige} - Q_{in\_kg}}{\rho} \cdot \left(r_{casing}^2 - r_{hub1}^2\right) \cdot \pi$$

Expressed in *m/s*.

- Main outlet velocity (without injected mass flow):

$$V_{x2} = \frac{q_{corrige} - Q_{in\_kg}}{\rho} \cdot \left(r_{casing}^2 - r_{hub2}^2\right) \cdot \pi$$

In *m/s*.

New pressure rises were calculated as follows:

- Total to static pressure rise, without injected mass flow:

$$P_{rise\ t-s} = P_{s-s} - \frac{1}{2} \cdot \rho \cdot V_{x1}^2$$

In *Pa*.

- Total to total pressure rise, without injected mass flow:

$$P_{rise\ t-t} = P_{s-s} + \frac{1}{2} \cdot \rho \cdot (V_{x2}^2 - V_{x1}^2)$$

Evaluated in *Pa*.

- New flow coefficient, without injected mass flow:

$$\Phi = \frac{V_{x1}}{U}$$

Which is dimensionless.

- Total to static pressure coefficient:

$$\Psi_{t-s} = \frac{P_{rise\ t-t}}{\frac{1}{2} \cdot \rho \cdot U^2}$$

That is dimensionless.

At this point, program *interface_soufflage_bis* takes the last stability point data from the *control* cases, which is, as discussed previously, the penultimate value, until the last one is already in stall conditions. In particular, program takes the last stability mass flow point, which enables to evaluate a parameter for the improving conditions obtained with air injection.

The next parameter allows to compare different configurations and clearly shows the best one; it is called *Stall Margin Improvement (SMI)*. In order to compute it, it's necessary, firstly, to evaluate the *Stall Margin (SM)*. There are different ways to evaluate it but, that one used by the author and PhD student Gabriel is reported below:

- *Stall Margin*:

$$SM = \left[\left(\frac{P_{rise\_t-t}}{q_{corrige}} - \frac{q_{corrige\ nom}}{P_{rise\_t-t\ nom}} \right) \cdot \frac{P_{rise\_t-t\ nom}}{q_{corrige\ nom}} \right] \cdot 100$$

$$= \left(\frac{P_{rise\_t-t}}{q_{corrige}} \cdot \frac{q_{corrige\ nom}}{P_{rise\_t-t\ nom}} - 1 \right) \cdot 100$$

This quantity is dimensionless and expressed in percentage; $q_{corrige\ nom}$ is the nominal corrected mass flow, for *no control case*, at *3200 RPM* and it's equal to *5.3 kg/s*, while $P_{rise\_t-t\ nom}$ is the nominal total to total *no control* pressure rise at the same rotational speed, equal to *3600 Pa*.

So, for each stability point, it's possible to compute the *Stall Margin*; in particular, what is interesting, is to evaluate the *SM* for the last stability point for each data file. In this way a list of latest stability points it's obtained, each referring to a different pressure or injectors configuration, but with the same injection angle configuration. Therefore, it is possible to evaluate the gain passing from the baseline configuration, that is *no control* case, and all the other ones. To do this, finally the *SMI* is calculated:

- *Stall Margin Improvement*:

$$SMI = \frac{SM_i - SM_{baseline}}{SM_{baseline}} \cdot 100$$

Where the SM_i refers to the stall margin calculated for each type of control configuration and the $SM_{baseline}$ stands for the stall margin of the *control case*. Like the *Stall Margin*, it's a dimensionless number, expressed in percentage.

Another way to evaluate the *Stall Margin Improvement* is reported below:

- Mass flow *Stall Margin Improvement*:

$$SMI_q = \frac{q_{corrige\ 1} - q_{corrige\ i}}{q_{corrige\ 1}} \cdot 100$$

Where $q_{corrige\ 1}$ is the last stability point corrected mass flow for the *no control case* (the so called *baseline*), while $q_{corrige\ i}$ is the last stability point corrected mass flow for the *control case*; SMI_q is a dimensionless number as *SMI*.
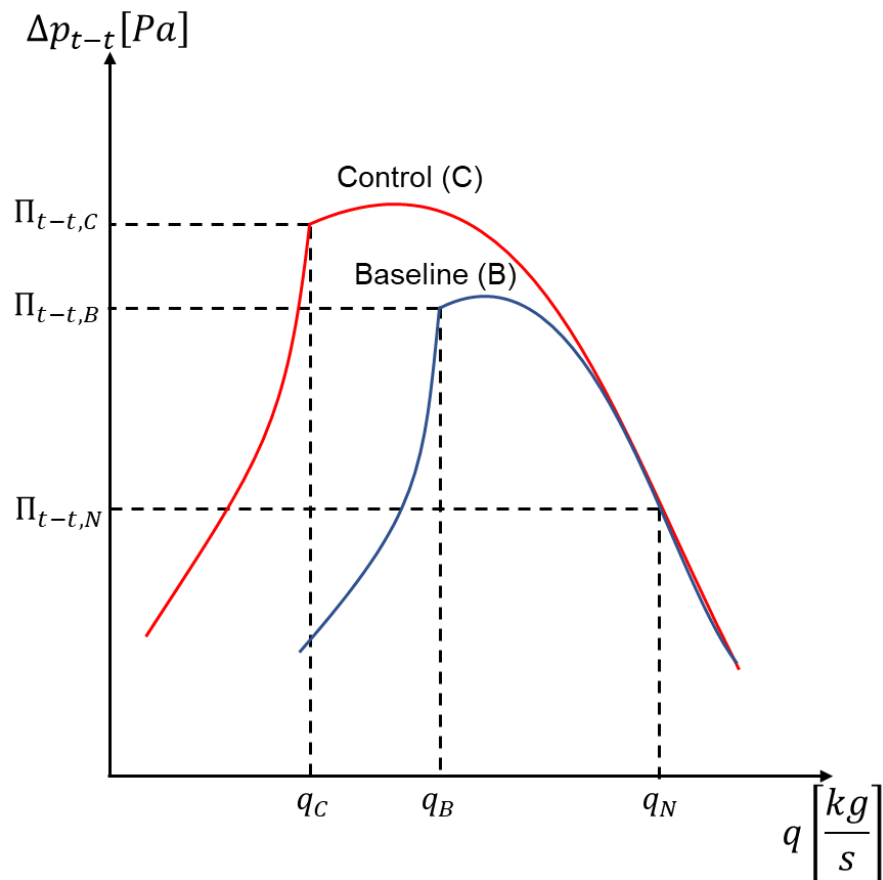

Figure 24: Representation of parameters involved in computing SMI

The difference between the two is that the first type of *SMI* takes into account both the pressure gain and the mass flow rate, while the second one compares only the mass flow rate of the *control* and *no control* cases. For more, the first one considers also the compressor's nominal conditions at the specific rotational speed. For these reasons, the first one, *SMI*, is more complete and will be used instead of SMI_q.

Together with *SMI*, the program allows to evaluate the pressure gain that is defined as follows:

- Pressure Gain:

$$Gain\_P = \frac{P_{rise\_t-t\ i} - P_{rise\_t-t\ 1}}{P_{rise\_t-t\ nom}} \cdot 100$$

Where $P_{rise\_t-t\ I}$ is the total to total pressure of the last stability point for control system's data, $P_{rise\_t-t\ 1}$ is tthat one of the control system and $P_{rise\_t-t\ nom}$ is the nominal total to total pressure rise for the *no control case*, equal to *3600 Pa*. The value is expressed in *Pa*.

Another important parameter the program provides, is the energy gain; practically it evaluates how much energy is gained by the air in *control case* with respect to the *no control one*, considering both the pressure increasing and the mass flow reduction.

- Energy Gain:

$$Gain\_NRJ = \frac{q_{corrige\ 1} \cdot P_{rise\_t-t\ 1}}{\rho_1} - \frac{q_{corrige} \cdot P_{rise\_t-t}}{\rho}$$

Where the subscript *1* refers to quantities concerning last stability point for *no control case*, while the other ones refers to quantities concerning last stability point for *control cases*. This quantity is expressed in *J* as mass flow rate, pressure rise and density are respectively computed in *kg/s*, *Pa*, and *kg/m^3*.

Anyway, with this type of approach, energy spent in the screw compressor to store compressed air in the tank, is not considered; so, it's necessary to compute this energy and compares it with the energy gain active control gives to compressor. To do so, kinetic energy of air stream coming from injectors is approximately evaluated.

- Air injected kinetic energy:

$$Cout\_NRJ = \frac{1}{2} \cdot \rho \cdot \frac{Sinj}{Nb_{EV}} \cdot V_{in}^3$$

This expression is evaluated in *J*;

Finally, it's possible to evaluate the energy balance between the pressure and mass flow gain and the kinetic energy injected air gains.

- Energy balance:

$$Bilan\_NRJ = Gain\_NRJ - Cout\_NRJ$$

Where all quantities are in *J*.

5.1.2   Interface

As this program was built on Matlab GUI, what it is possible to see once it is launched, is the interface presented in Figure 23. On the left part there's a table list in which there are several data files labelled in different way corresponding to the three main configurations (*7.5 bar, 10 injectors and 20 injectors*). Next to it there a small box labelled as *Actions* in which there are several buttons:

- *Plot perfos*: it allows to create a graph plotting the compressor characteristic curve; the chart is created in the left graph. To plot it, it's necessary to select some data files in the left table list, always including the *no control* case, and push *plot perfos* button; once done the graph appears and the table in the bottom part of interface is filled;
- *Plot gain*: when table in the bottom part is filled, it is possible to select two of the columns and fill the right plot with a new graph with these two new set values parameters;
- *Clear* (left one): allows to clear the left graph;
- *Clear* (right one): allows to clear the right graph;
- *Invert*: this button allows to change, in the right plot, the x-axes values with the y-axes ones.

Immediately below these five buttons there are two windows menus, in which it's possible to select the kind of x- or y-axes to plot in the left graph; particularly the first one allows to change the x-axes and has two options:

- *q*, the overall mass flow inside compressor;
- *Phi*, the flow coefficient.

In the second one there are six options in the window menu:

- *Delta p_{s_s}*, the static to static pressure difference;
- *Delta p_{t_s}*, the total to static pressure difference;
- *Delta p_{t_t}*, the total to total pressure difference;
- *Psi$_{s\_s}$*, the static to static pressure coefficient;
- *Psi$_{t\_s}$*, the total to static pressure coefficient;
- *Psi$_{t\_t}$*, the total to total pressure coefficient;
- *Puissance étage*, the stage power;

The table placed in the interface bottom part contains several parameters, most of them have been described in 5.1.

5.2 "SUPER_PROGRAMMA"

"Super_programma.m" was a program built by the author to collect all together data for each test done. Firstly, data had to be well labelled because program take automatically all data files in the order they are listed. Secondly, for each data file, this program detects the penultimate point, which is the so called *last stability point*, and store each parameter belonging to this point; thus, there will be different vectors, like pressures or velocities, and each element of them will represent the specific parameter for a specific configuration, at its last stable point.

5.2.1 Calculations

Calculations were the same as done in 5.1, there are only two differences between the programs: injection velocity and energy balance calculations.

5.2.1.1 Injection velocity

To evaluate it, firstly, the exit air injected temperature is estimated:

$$T_e = \left(T_{tampon} + 273.15\right) \cdot \left[\frac{P_{atm}}{\left(P_{tampon} + 1\right) \cdot 10^5}\right]^{\frac{\gamma-1}{\gamma}}$$

Where *T_{tampon}* is in *°C*, *P_{atm}* in *Pa*, *P_{tampon}* in *bar*, *γ* is equal to *1.4*; the *+1* in the bottom part of fraction is due to the fact that the pressure inside the small vessel (*P_{tampon}*) is relative to the atmospheric one, that is, approximately, equal to *1*.

Once it is evaluated, it's possible to compute the air density coming from the injection system.

$$\rho_e = \frac{P_{atm}}{R \cdot T_e}$$

Where R is the universal specific gas constant equal to *287.05 J/(kg*K)* and ρ_e is expressed in *kg/s*. Both T_e and ρ_e are vectors containing respectively last stability point's temperature and density. Finally, it's possible to evaluate the injection velocity:

$$V_e = \frac{Q_{in}}{\rho_e \cdot Sinj \cdot DC}$$

Where V_e is in *m/s* and *Sinj*, *DC*, Q_{in} are parameters already presented.

5.2.1.2 Energy gain

Instead of computing the energy gain in the last stable point for the specific control case and in the *no control* one, it had been evaluated comparing the last stable point in the *no control* case and a point with the same mass flow rate with the corresponding total to total pressure rise.

To do so, it had been used the default Matlab function *interp1*; putting inside the *control* total to total pressure rise and mass flow rate, together with *no control* mass flow rate and the option *"spline"* it was possible to obtain the *control* total to total pressure rise corresponding at the same *no control* mass flow rate.

Once the new pressure rise values are calculated, then the following calculations are the same done in the last part of 5.1.1.2.

5.2.2 Output graphs

When program is launched, it takes several minutes to compute everything and to give the desired output; as results it is obtained a series of graph, in which all five injection angle configurations are compared. Particularly:

- *SMI* as a function of *Injection Angle* for *10 blocks* and *5* different injection pressure;
- *SMI* as a function of *Injection Angle* for *20 blocks* and *5* different injection pressure;
- *SMI* as a function of *Injection Angle* for injection at *7.5 bar* and *6* different injectors configurations;
- *Energy Balance* as a function of *Injection Angle* for *10 blocks* and *5* different injection pressure;
- *Energy Balance* as a function of *Injection Angle* for *20 blocks* and *5* different injection pressure;

- *Energy Balance* as a function of *Injection Angle* for injection at *7.5 bar* and *6* different injectors configurations;

- A 3D plot representing *SMI*, *Injection Angle* and *Injectors number* for injection at *7.5 bar*;

- *SMI* as a function of *Injection pressure* for *10 blocks* and *5* different injection angle configurations;

- *SMI* as a function of *Injection pressure* for *20 blocks* and *5* different injection angle configurations;

- *SMI* as a function of *Injectors number* for injection at *7.5 bar* and *5* different injection angle configurations;

5.3 "INTERFACE_BIS"

"interface_bis" is a Matlab GUI program built by PhD student Gabriel and allows to process all the big data amount coming from pressure field tests. Firstly, before use it, it's necessary to launch *CalculCorrelationAutomatique*, which enables to create several correlations that *"interface_bis"* needs in order to treat data.

On Figure 25 it's possible to have a look at the main program interface; once it is launched, in the right side it will be possible to see a red highlighted written because a data file hasn't been charged yet. In this case, the written is highlighted in green that means that the data file has been correctly upload.

To upload a file, it's sufficient to push the button *charger* on the right side of the picture; a pop-up window will appear and it will be need to select the data file named as *data*, which is present in each test folder. When selected, the highlighted written will become yellow until the program has load the file; once it has, it will turn into green.

On the left hand side of Figure 25 there are four different graphs; they are blank once the program is launched, but then they fill in when data file is correctly load; in particular, all of them have the same x axes which refers to the test's duration time. The top, the third and the bottom graph was never used by the author. In the second one, it's possible to see the unfiltered (that means that it contains the blade frequency) pressure trend.

On the central part of the snapshot, it's possible to see three different list tables, and three other different boxes:
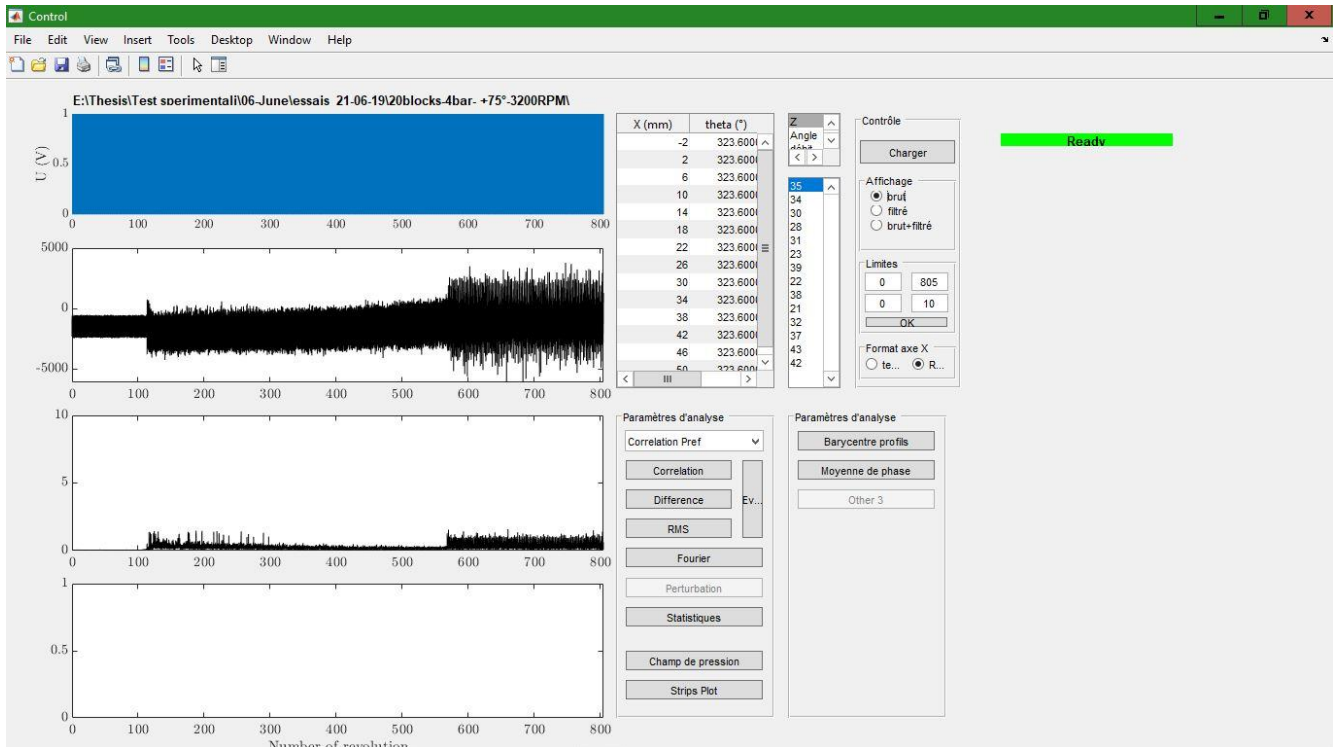
Figure 25: "interface_bis.m" main interface

- The first list table presents the *16* different pressure probes, and for each of them, it's reported the axial distance with respect to blades leading edge, the angular position where they are placed (*0°* is set at the top part of compressor, and the rotation is counter-clockwise) and a number which refers to each of them;

- The second one allows to change the y-axes parameter displayed in the first of fourth graphs; options available are *Z* (the graph obtained presents a flat zero trend and, corresponding to each rotor revolution, a bump), *Angle* (shows the angular distance of a blade taken as a reference, from the compressor top point, as for pressure probes), *debit* (mass flow rate) and *Variation* (which was never taken into account);

- The third one refers to pressure probes, which are listed starting from the first one that sees the mass flow, up to the last one; each of them has a specific number that distinguished them;

- The first box, the centre left top ones, labelled as *contrôle* has four different parts: on its top, it's possible to find *charger* button that has been already presented; then, there's a section named *Affichage*, where it's possible to change the type of pressure traces in the second plot on the left hand (*brut* stands for unfiltered pressure, that is pressure trend including blades frequency; *filtré*

stands for pressure trend filtered from blades frequency and finally *brut+filtré* represents both filtered and unfiltered pressure trend); after that, there's the *Limites* section, in which is possible to change the x-axes time lapse and the y-axes range (changing x-axes, all four plots are changed, while changing the y-one, it changes only the selected graph) and finally, in the bottom section, it is possible to change the x-axes unit, choosing from time, in *s*, or rotor revolution, *RPM*;

- The second one, labelled *Paramètres d'analyse*, presents several buttons and one window menu; the author doesn't know at what they refer to, but the only two that has been used were the last ones: *champ de pression* and *strips plot*, about which it will be discussed below;

- Then, the last box, named *Paramètres d'analyse*, has never been used.

5.3.1 "champ de pression"

When *"champ de pression"* button is pushed, immediately a pop-up window appears (left of Figure 26). It asks the graph format; it has been always used the second option, *1D (Z) + temps*, which allows to create a mesh plot, comparing the pressure probes axial distance from blades leading edge (in the y-axes) and acquisition time (or rotor revolution) in the x-axes.
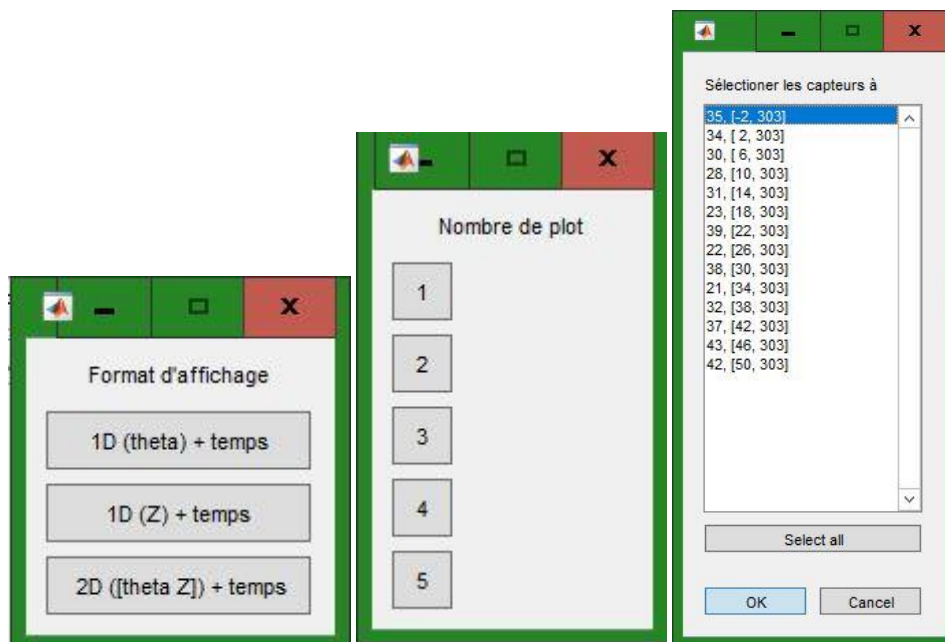

Figure 26: The 3 consecutive pop-up windows appearing once pushed "champ de pression button"

Then, another pop-up window appears (centre of Figure 26), which asks the number of plots desired; it has always used 1 plot. After having pushed it, another pop-up window appears in which is possible to select

which pressure probes to plot; lot of combinations are available, but in this work, it had always used all of them.

Finally, *"Champ de pression"* interface appears (Figure 27); the main part of it, is composed by a colormap graph in which different pressure levels are plotted inside graph. On the y-axes, it's presented the axial distance from blades leading edge; as described in Figure 15, each probe is placed *4 mm* far from the previous one. On the x-axes, the reference is the time test duration; it could be in *s* as reported in the figure below, or in *RPM* depending on how it has been formatted the axes before (see Figure 25). On the right hand side of interface, a pressure colour bar is present in order to be able to see how pressure evolves throughout the whole test.
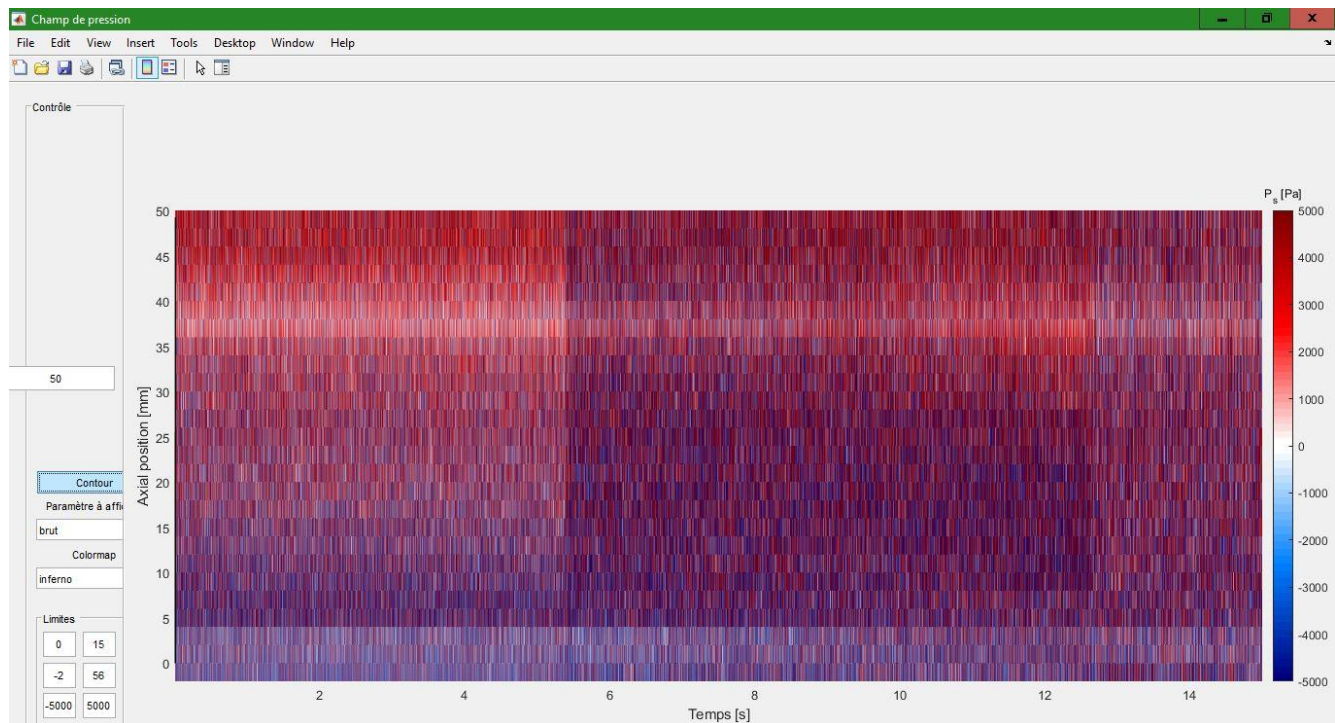

Figure 27: "Champ de pression" interface

On the right hand side of the plot, there are some other options that can easily help the user. *Contour* option button allows to export the entire plot or a part of it, depending on the limits imposed in the x and y axis, to a Matlab figure window; *Paramètre a affichage* allows to change pressure type choosing between *brut*, *filtré* or *brut + filtré*, as described previously; *colourmap* permits to change colour of the pressure map plot, and *Limites* allows to change respectively x-axes, y-axes and pressure range. In the case presented here in Figure 27, the

colour map selected is the blue white red one; red colour means positive pressures, blue one means negative ones, and white one means zero pressure; obviously, all these pressures are relative to the atmospheric one.

5.3.2 "strips plot"

With *"strips plot button"*, it is possible to create plots representing the pressure trend for each, all or some of the pressure probes; once it is pushed, a first, of five pop-up windows, appears. In the first one, it will be asked how many plot are desired, from *1* up to *5*; then a second one will demand the pressure type to be plotted (*brut*, *filtrè* and *brut + filtrè*); after that the third one will ask if to plot the pressure probe axial position; the fourth one will demand if to plot the blades (actually this option is not working properly, so it doesn't matter if *oui* or *non* are chosen); finally, the last pop-up window will ask which pressure probe trend to plot, and it will ask as many times as the number of plot chosen in the first pop up window (Figure 28).
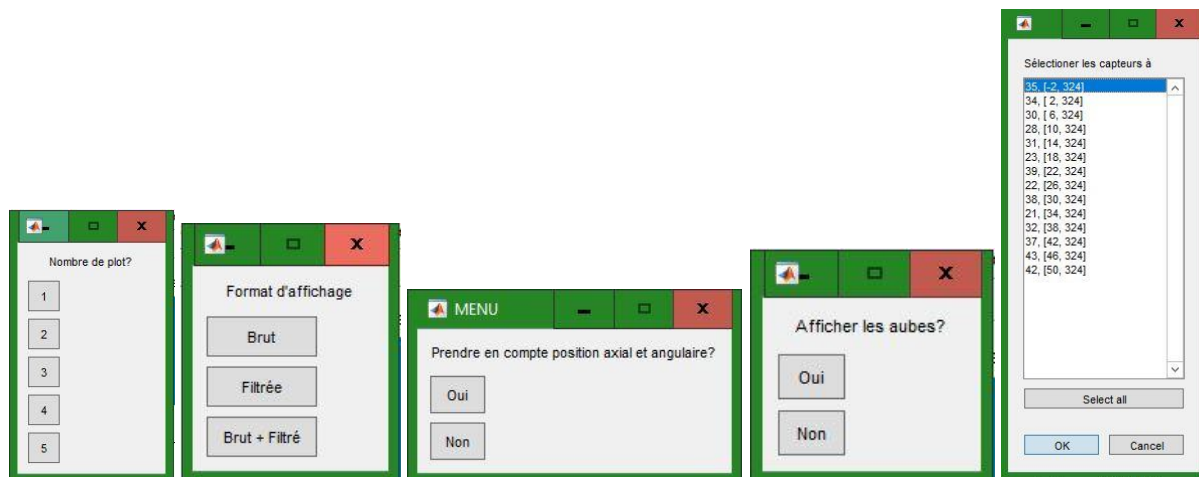

Figure 28: The 5 consecutive pop-up windows appearing once pushed "strips plot" button

In the end, when all these passages are completed, pressure trend plot will appear; the graph (see Figure 29) presents pressure trace as a function of the number of rotor revolution. In case presented below, unfiltered pressure is drawn in black while filtered one in red. Two bumps are clearly visible in the plot; the first one, at almost *300 RPM* is when the injection is activated, while the second one is when compressor reach rotating stall.
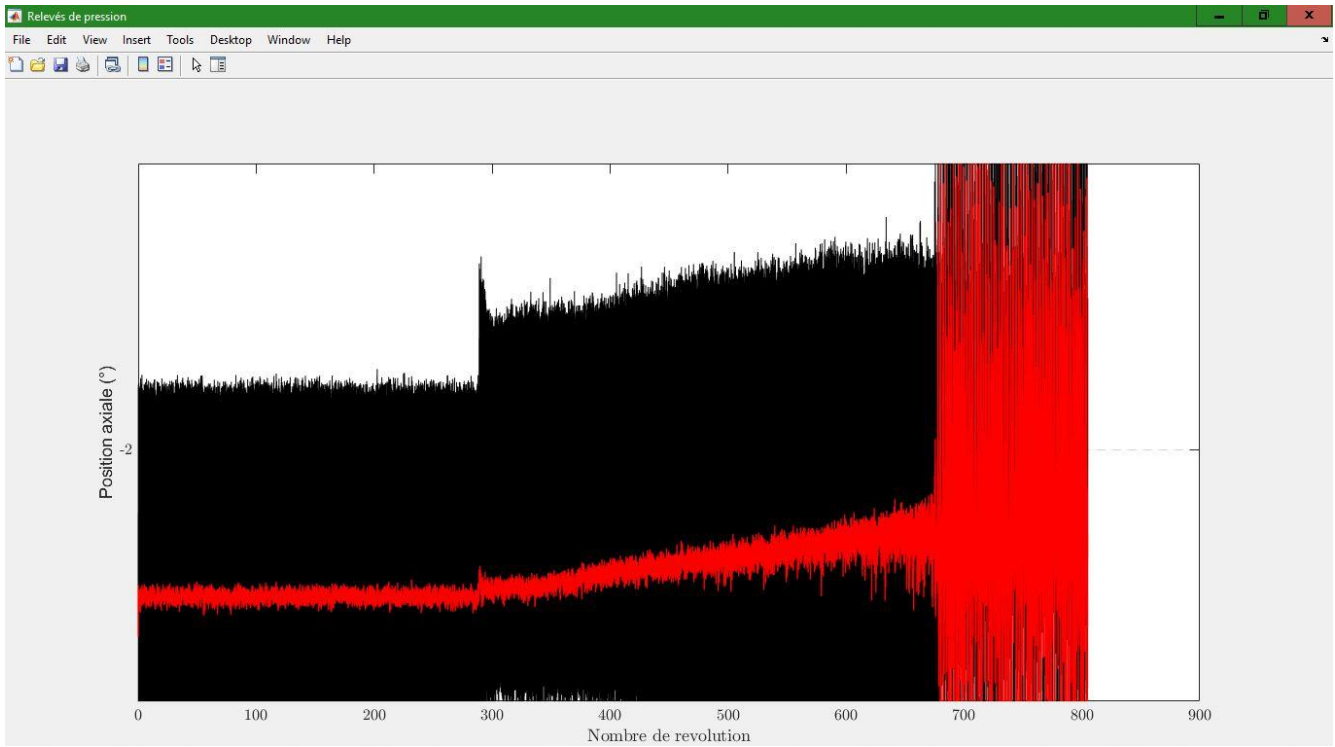
63

Figure 29: "strips plot" graph interface

6 RESULTS

As discussed previously in chapter 5, the first part of this work was about finding the best injection angle configuration and the second one was about looking at what's happening inside compressor stage while injecting air at different injection angle. So, the first part of this chapter will present results concerning the best configuration while the second one will be about pressure behaviour inside compressor stage.

6.1 BEST INJECTION ANGLE CONFIGURATION

6.1.1 SMI-injection angle

Here are presented results comparing the *SMI* as a function of *injection angle* for different configurations:

- Figure 30 presents its trend for *10* injectors blocks on, with five different injection pressures;
- Figure 31 shows the same as figure 28, but for *20* injectors blocks on;
- Figure 32 represents the same as the previous two, but what remains constant is the injection pressures, at *7.5 bar* for different injector blocks on.
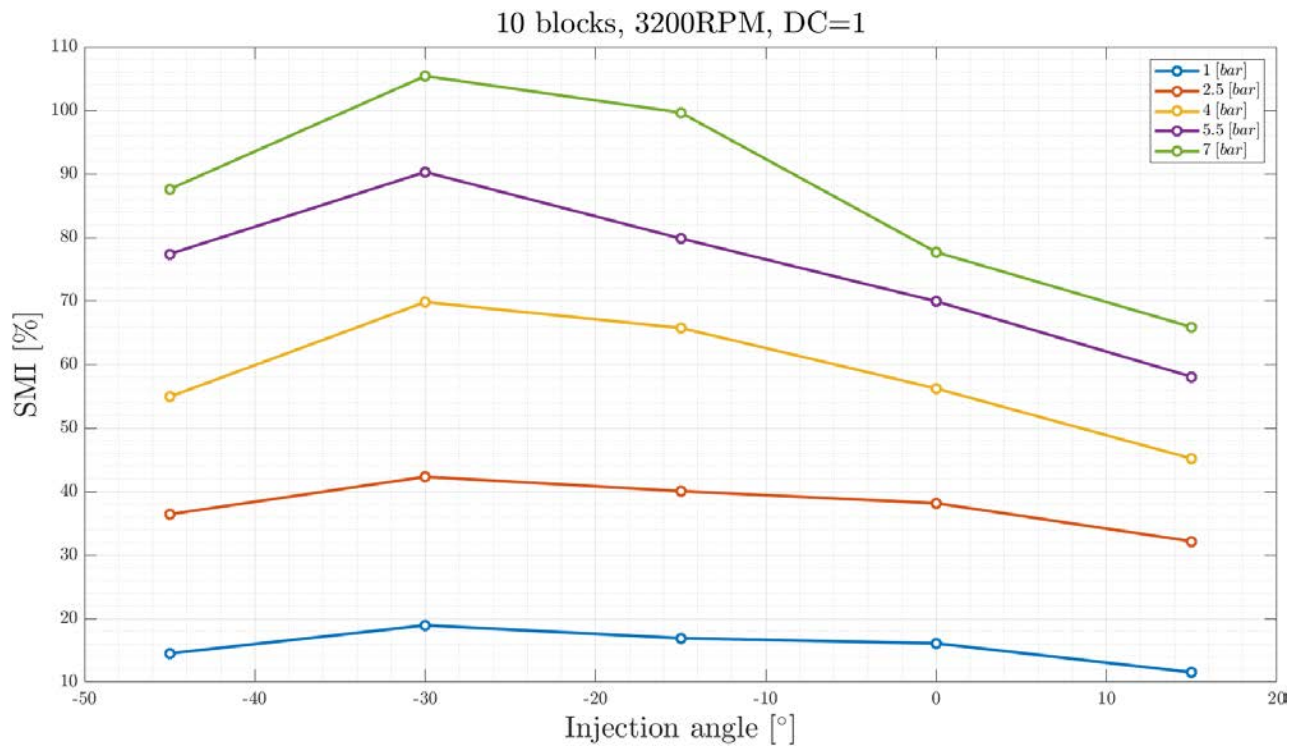

Figure 30: SMI as a function of injection angle for 10 blocks, 3200 RPM and DC equal to 1 and different injection pressures
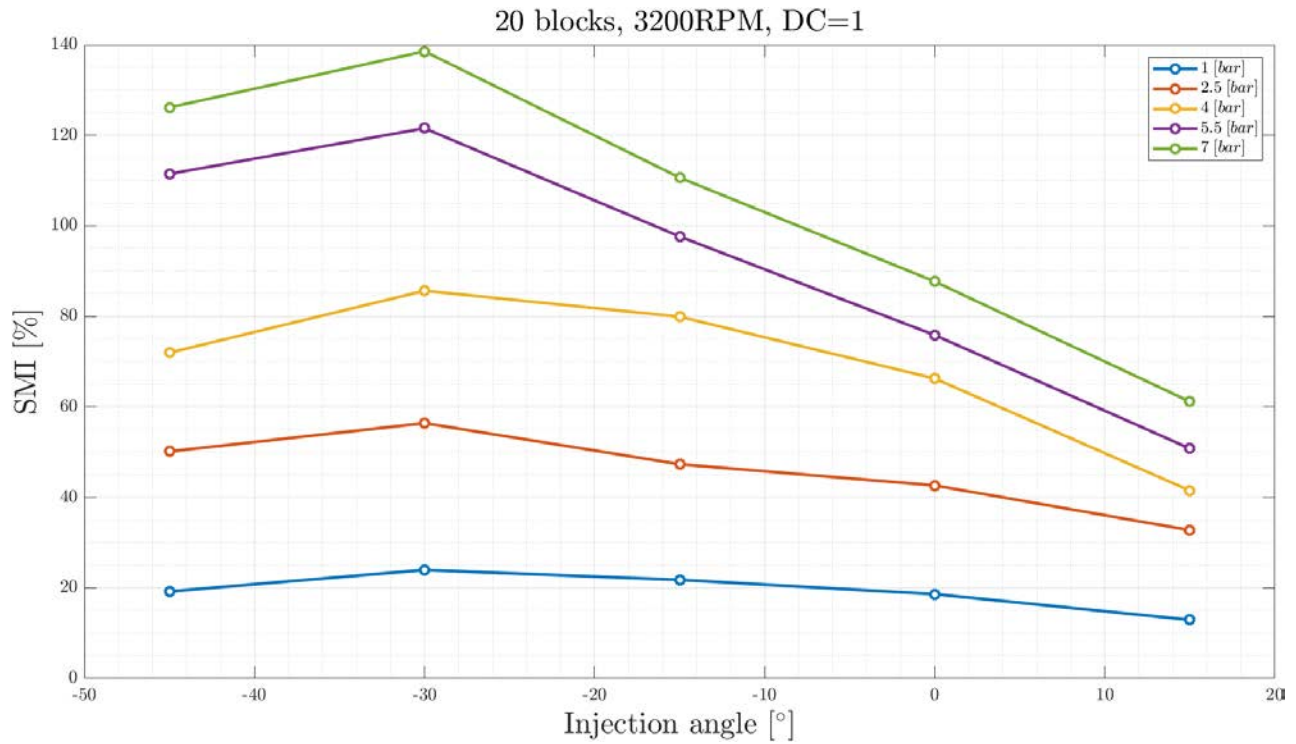
Figure 31: SMI as a function of injection angle for 20 blocks, 3200 RPM and DC equal to 1 and different injection pressures
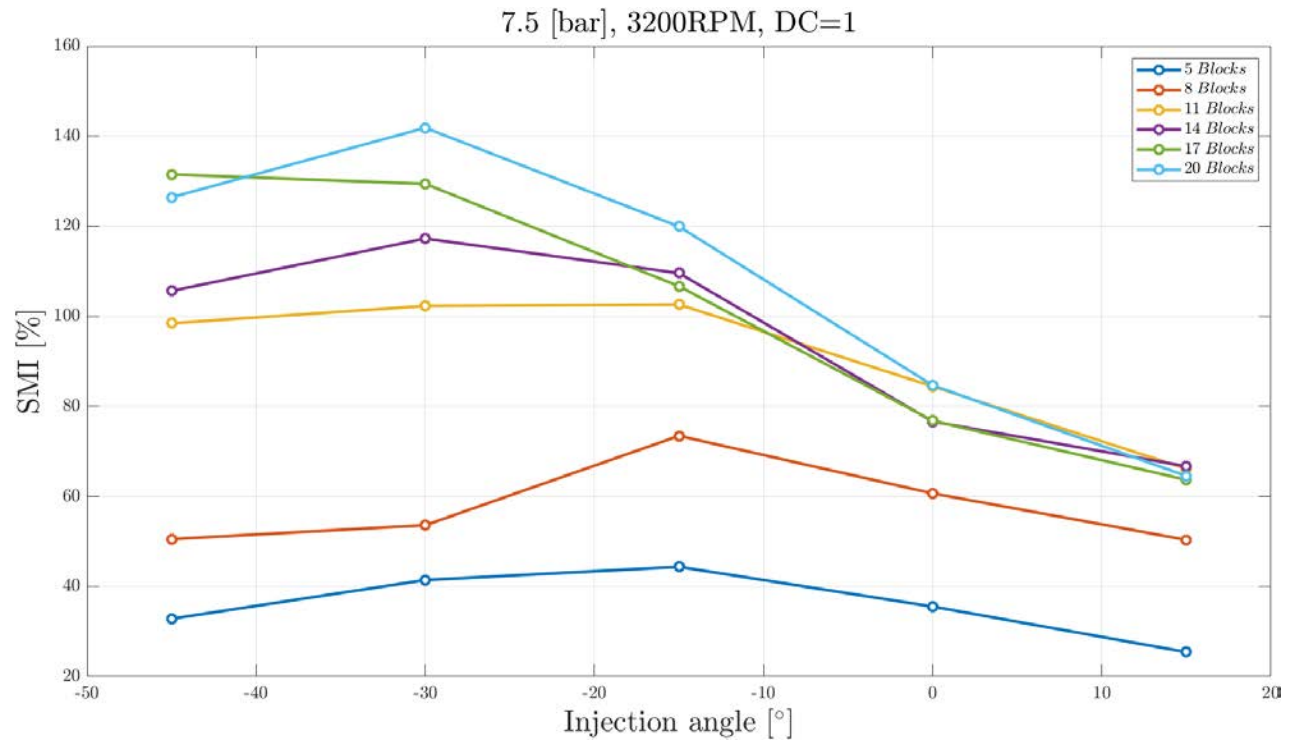

Figure 32: SMI as a function of injection angle for 7.5 bar injections, 3200 RPM and DC equal to 1 and different injector configurations

Concerning Figure 30 and Figure 31 some particular things can be pointed out:

- For both graphs, the best configuration is at *30° injection*;
- For low injection pressure the *SMI* tends to be very close between different injection angle configurations; *SMI* curves tend to be flatter for *1* and *2.5 bar*. On the contrary, for *4*, *5.5* and *7 bar* injection pressure, the *SMI* trend is very marked and a maximum is clearly visible;
- *20 blocks* configuration is clearly better than *10 blocks* one, and this is quite obvious; all injectors on, covering all the compressor circumference are a better solution than half of them covering the same space. Anyway, looking carefully at these graphs, it could be seen that the *+15°* injection angle configuration, works better for *10 blocks* on rather than *20 blocks on*, when the injection is set at *4*, *5.5*, and *7 bar*. Probably this could be explained considering that this particular injection configuration is working increasing the blade attack incidence angle that is not the best layout to postpone rotating stall; nevertheless, this type of configuration is not extremely bad and the positive effect on the *SMI* could be brought back to the high momentum injected in the compressor stage by the high pressure (and so high speed) air pumped in.

Regarding Figure 32, it can be pointed out that:

- There isn't a best configuration set up which is common to all the *6* different injection configurations; for few injectors on, in particular for *5*, *8* and *11 blocks* configurations, the best injection angle is at *15°* while for more injectors on, particularly for *14*, *17* and *20 blocks* configurations, the best is at *-30°* (for *17 blocks* configuration, the best configuration is at *-45°* but it could be considered as a mistaken data taken);
- There isn't also a best configuration in terms of injectors configurations at all; considering what was said in the upper point here, for *-45°, -30°, -15°,* and *0°* the best configuration is *20 blocks* on but for *+15°* it isn't. It seems that for angle which are not so favourable in terms of blade attack incidence angle, configurations with less injectors working are better; particularly, there's a clear difference between *5 blocks* and *8 blocks* and between these two and the rest, while for the other configurations, values are so close to each other;
- As pointed out for Figure 30 and Figure 31, the *SMI* trend tends to be flatter as the injection pressure is reduced; it means that, at high injection pressure, performances difference is very remarkable once the configuration is not the best one, while for low injection pressure, differences are minimal;
- There's a net difference between *5* and *8 blocks* with respect to other injectors configurations which is clearly visible for negative injection angle.

6.1.2 SMI-pressure

In this section, *SMI* trend is presented as a function of pressure for *10* and *20 blocks* configurations.

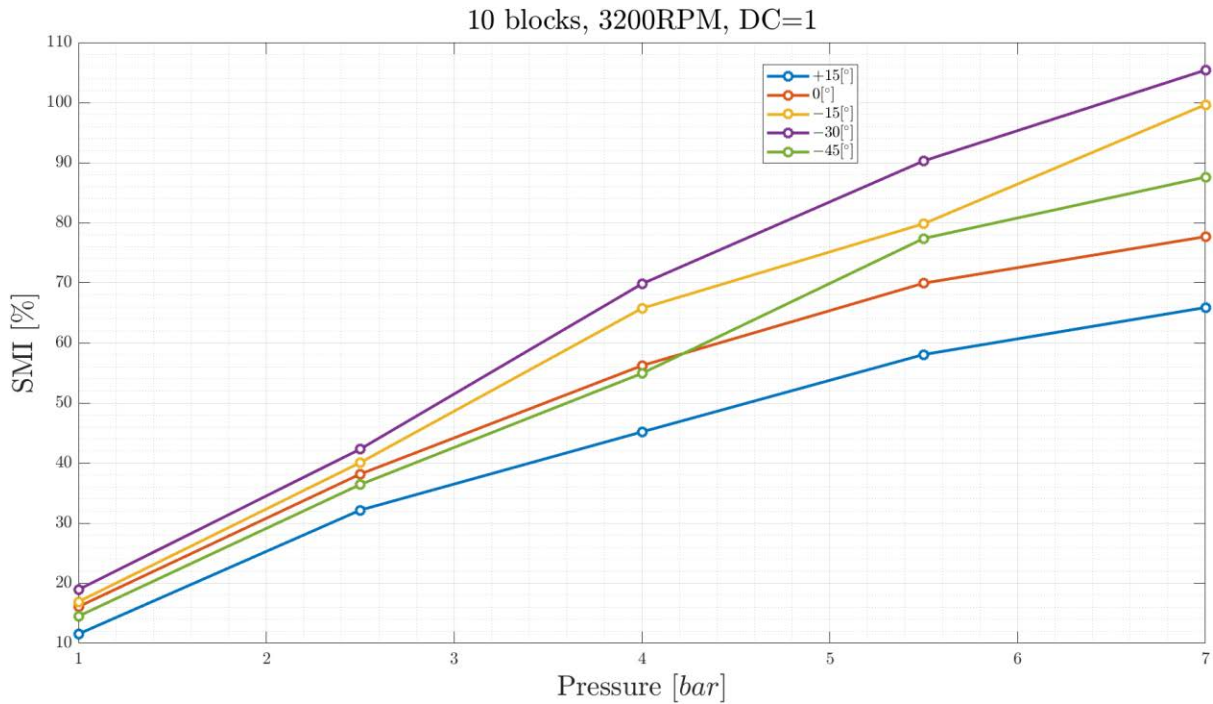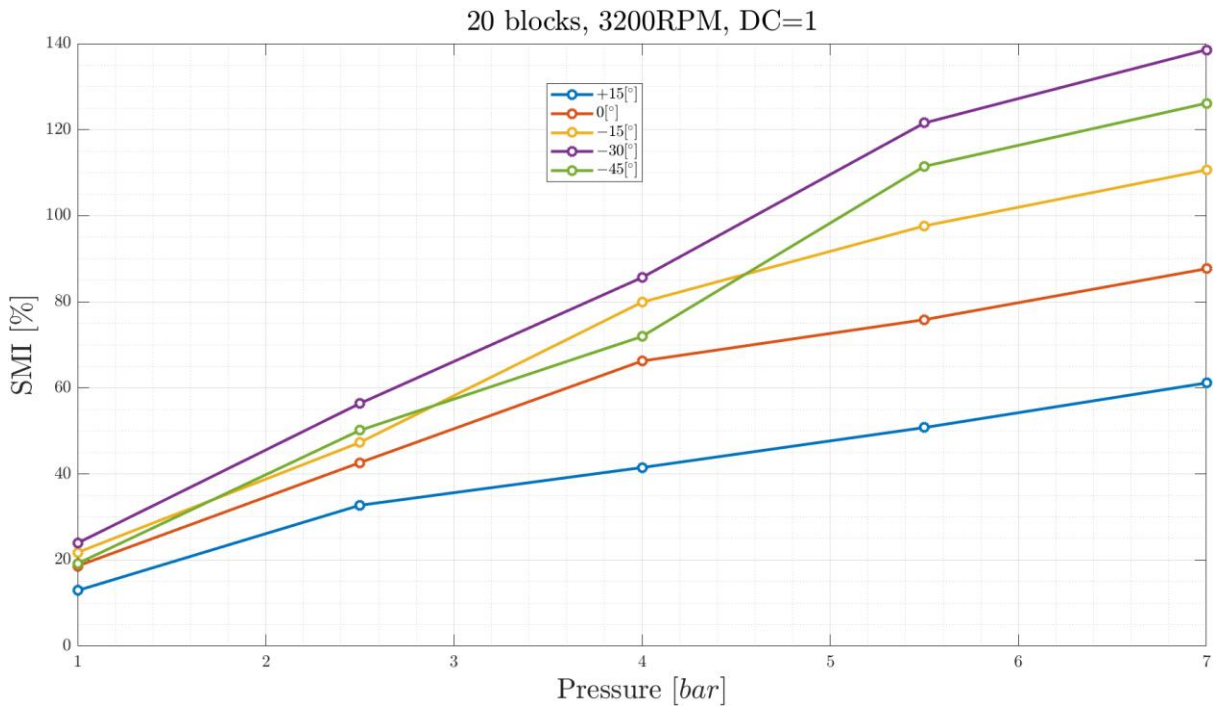*Figure 33: SMI as a function of pressure for 10 blocks, 3200 RPM, DC= 1 and different injection angle*

Figure 34: SMI as a function of pressure for 10 blocks, 3200 RPM, DC= 1 and different injection angle

- For both Figure 33 and Figure 34 the best injection angle configuration still remains *-30°* while the worst one still stays *+15°*;

- Comparing the single injection angle configurations between the two plots it's clear that *20 blocks* layout is always better than *10 blocks* one despite for *+15°* injection angle; here it is always worse than *10 blocks* for each pressure level but *1 bar*; as it was said before, probably at not favourable blade attack incidence angle, the entire compressor works better if the momentum injected is as much higher as possible;

- For *10 blocks* layout, *0°* injection is better than *-45°* one, at low injection pressure, up to *4 bar*, but after that *-45°* is better than it; for *20 blocks* layout, *0°* injection and *-45°* one, are very close to each other at low injection pressure, up to *4 bar*; but after that *-45°* is better than it;

- For *10 blocks* configuration, the second best configuration is *-15°* while for *20 blocks* layout, as described up here, there's no clear evidence which layout is the second best between *-45°* and *-15°* at low pressure;

- *SMI* slope tends to decrease in both graphs as the injection pressure increases; this could lead to think that the relationship between these two parameters could be a sort of quadratic type.
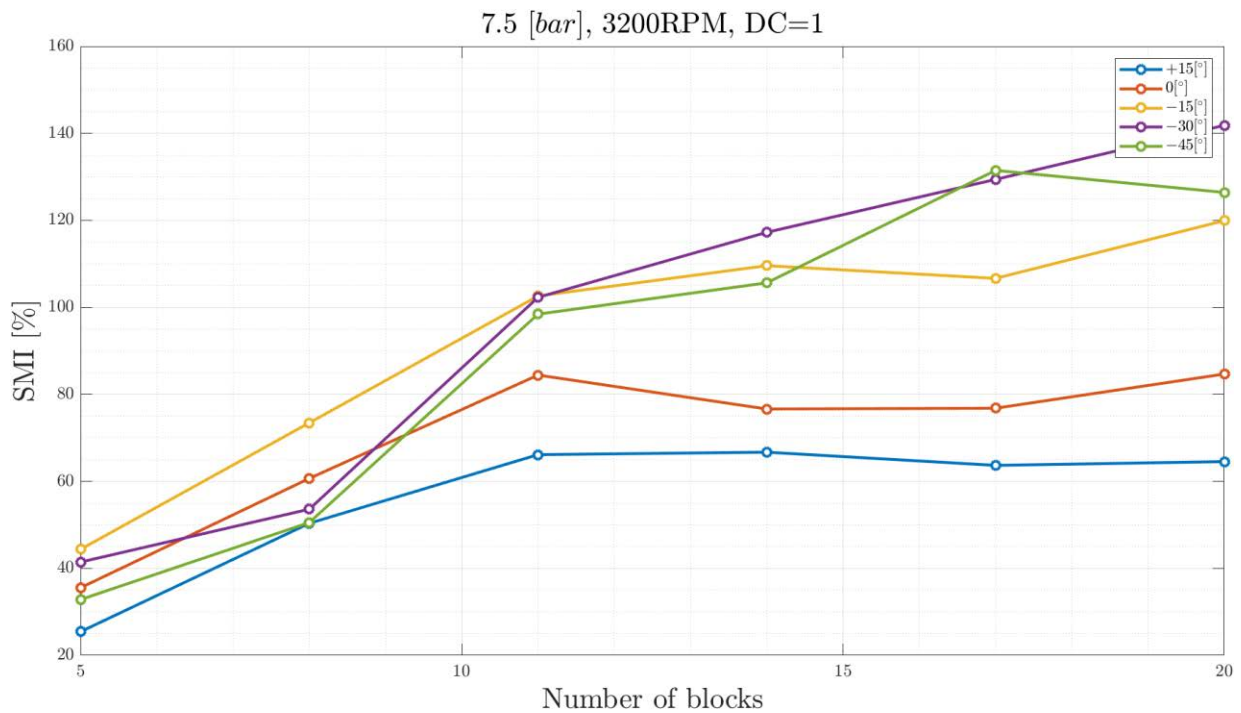
6.1.3 *SMI*-injectors number

Figure 35: SMI as a function of injectors layout for 7.5 bar, 3200 RPM, DC= 1 and different injection angle

69

Here, the *SMI* is plotted as a function of injector configuration. It's possible to see that:

- There isn't an injection angle configuration which is always the best with respect to the others; for *5, 8* and *11 blocks*, the best injection angle layout is *-15°* while for *14, 17* and *20 blocks*, the best one is *-30°*;
- The worst configuration is and still remains *+15°* for all injectors' configurations;
- *+15°, 0°* and *-15° SMI* trend, tend to increase (positive slope) from 5 up to 11 *blocks,* where it tends to be flat (slop close to zero); for the other two injection angle configurations, the slope tends to reduce but doesn't reach a value close to zero;
- The best injectors configuration for *+15°* and *0°,* is that one with *11 blocks* on, while for *-15°, -30°* and -*45°* the best one is the *20 blocks* working;

Figure 36 presents a *3D* graph, which takes into consideration contemporary *SMI, blocks number* and *injection angle*.
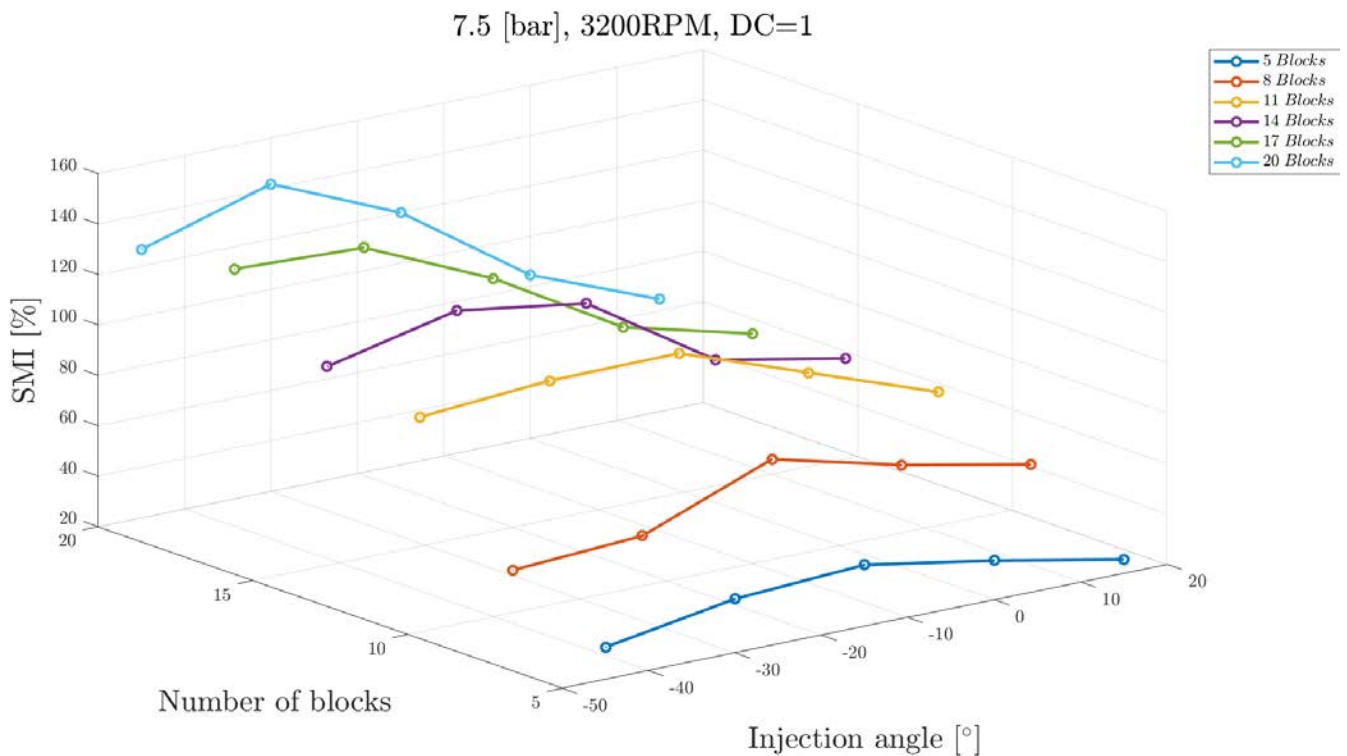

Figure 36: 3D SMI-blocks number-injection angle's graph for 7.5 bar injection, 3200 RPM and DC=1

6.1.4 Energy Balance-injection angle

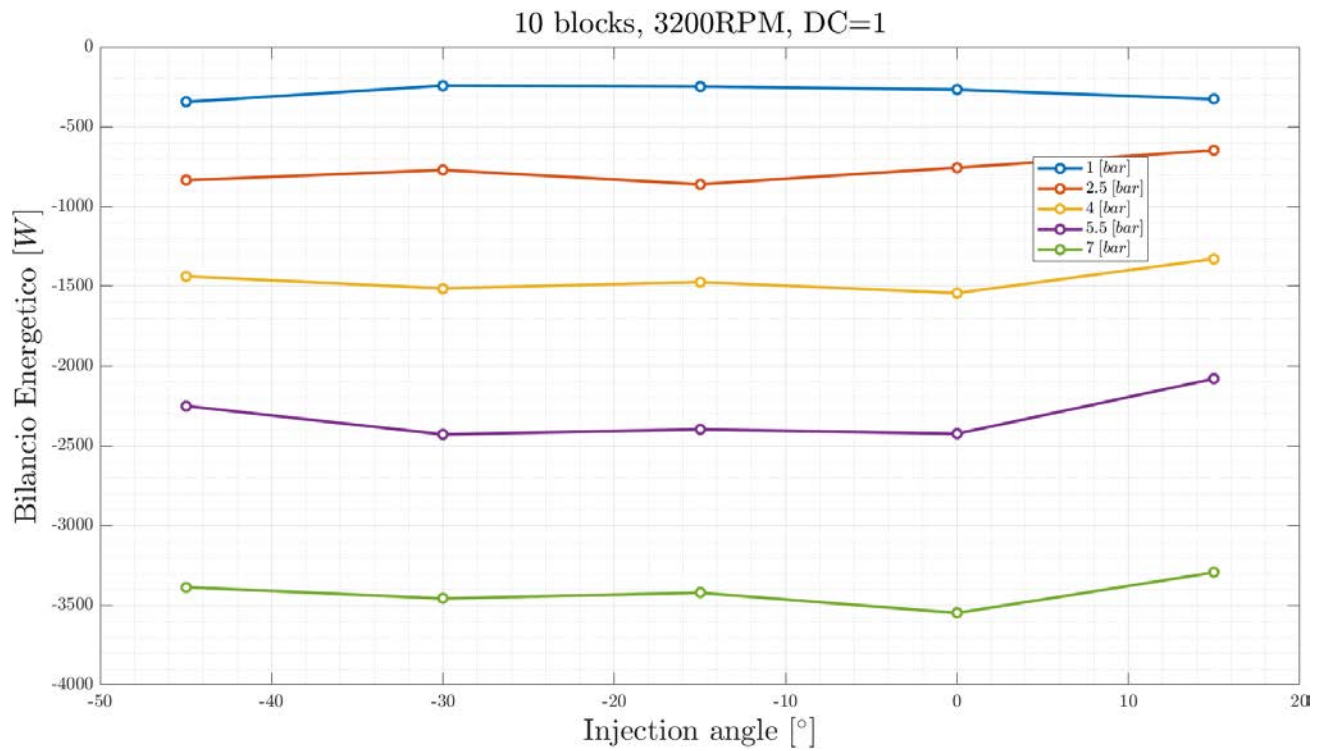Below energy balance as a function of injection angle's plot, are presented.

Figure 37: Energy Balance as a function of injection angle for 10 blocks on, 3200 RPM, DC=1 and different injection pressures
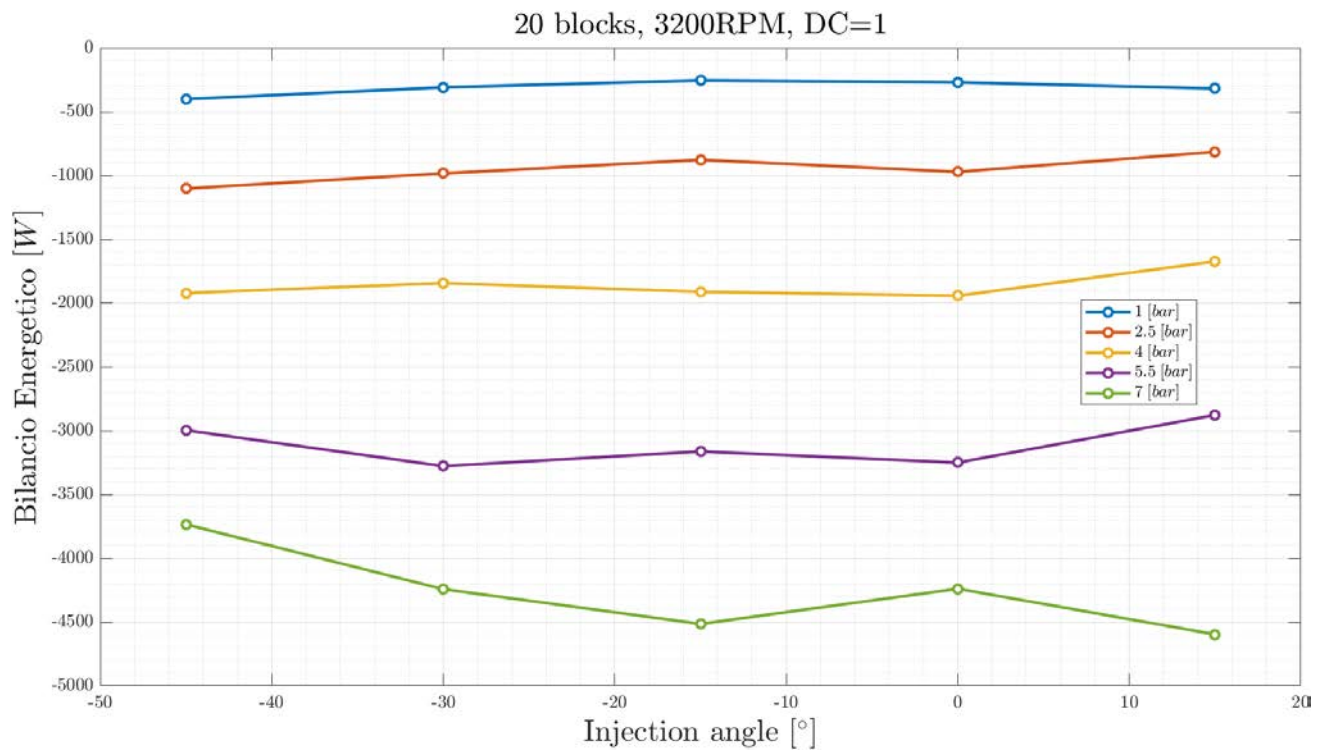

Figure 38: Energy Balance as a function of injection angle for 20 blocks on, 3200 RPM, DC=1 and different injection pressures
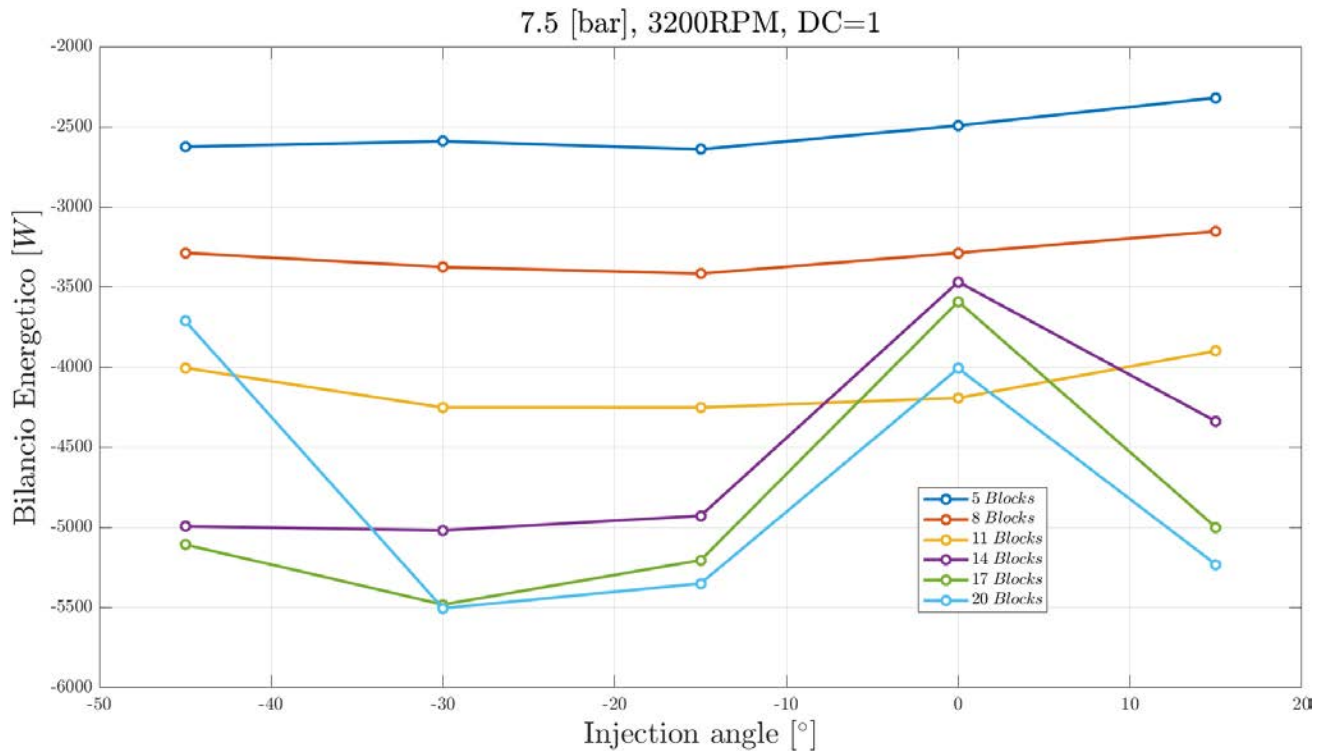
Figure 39: Energy Balance as a function of injection angle for 7.5 bar injection, 3200 RPM, DC=1 and different injectors layout

For Figure 37, Figure 38 and Figure 39, it is clearly visible that for each injection pressure, energy balance still remains more or less flat; it seems only that for *+15°* configuration, the energy balance tends to increase. Another important aspect to underline is that the energy balance is always negative; this means that injected air energy is higher than pressure gain obtained using this injection. Thus, this type of active control isn't energy saving but energy costing. Moreover, as injection pressure increase, energy balance becomes more and more negative.

These calculations are not so precise, as below is explained, but can give an idea of values and trends for injection energy consuming.

6.1.4.1 The injection speed problem

Figure 37, Figure 38 and Figure 39 shows the energy balance trend; to evaluate it, it had been used the two expression explained in 5.2.1.1. It has to be said, that these expressions used are not correct because it had been considered that air pressure in the two small tanks was not changed in the route from them to all injectors. But this is not correct at all; indeed, in the way air travel, from these two small tanks to injectors,

it met several turns and some narrowing that caused pressure drops; for more there were many entrance and outlet losses that caused pressure loss too.

Anyway, there were no other way to estimate injection speed because there wasn't any possibility of placing some hot wires just at the injectors exit, because it could be very dangerous for the compressor if one of them would have broken and fell into the compressor stage, causing very high damages to compressor rotor stage.

Another aspect to into consideration is that in expressions in 5.2.1.1 is that the outlet pressure used, is the atmospheric one; indeed, inside compressor, before reaching compressor stage, pressure inside is a little bit lower than the atmospheric one. However, it won't affect too much calculations done.

Some tests were made by *ONERA,* (as already shown in Figure 13) in order to see how injection velocity evolves in the space of *10 mm* which is the distance between injectors and compressor's blade (Figure 40).
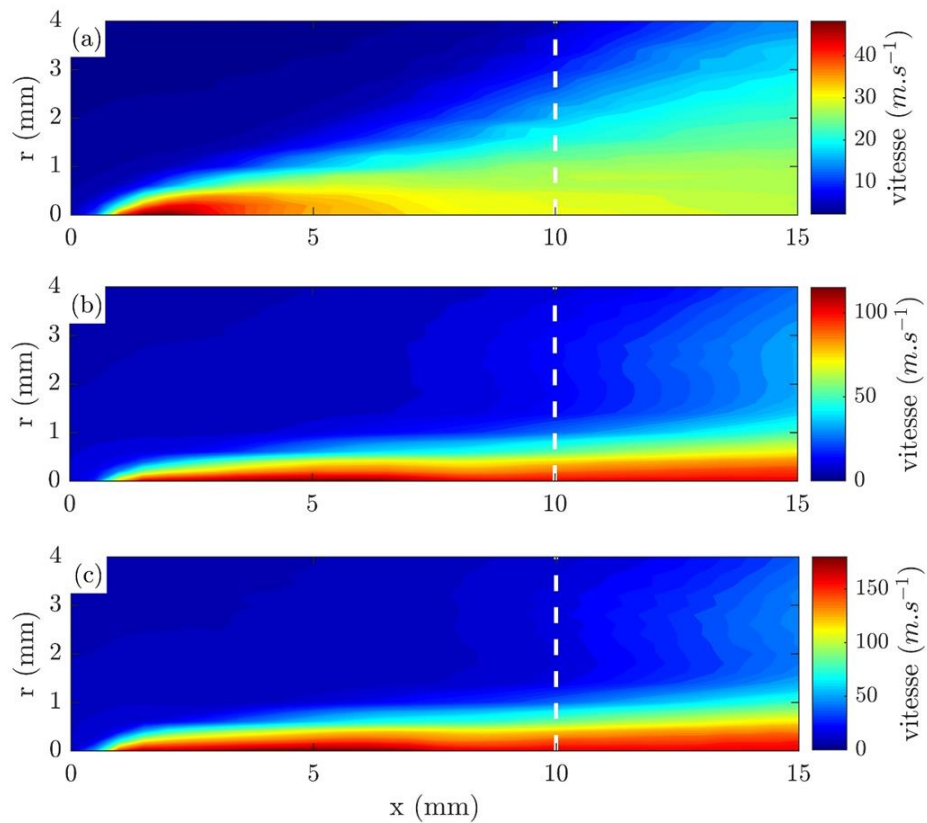

Figure 40: injection speed hot wire analysis by ONERA with three different mass flow: 20 L/min, 60 L/min, 100 L/min. In the x-axes is shown the jet length, in the y-axes the thickness

What it's clear from figure above is that, much more pressure the air jet has, much more the jet won't expand when blowing inside compressor encountering air it sucks. This means that at *10 mm* distance from injector exit, the velocity profile will be well defined ad with a reduced thickness.
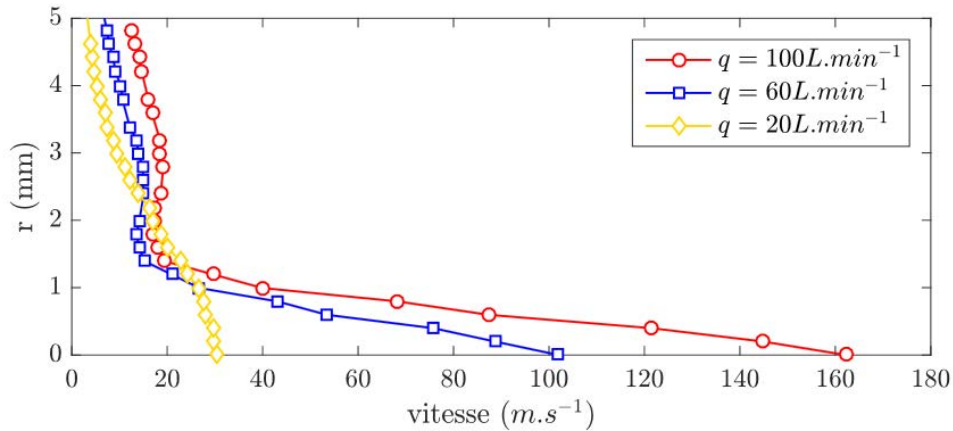

Figure 41: injection speed hot wire analysis by ONERA with three different mass flow: 20 L/min, 60 L/min, 100 L/min. Thickness as a function of jet speed

Above, in Figure 41, it is possible to see speed trend at varying of the axial injector distance; as the axial distance reduces, jet speed considerably increases when the mass flow increase. On the other hand, injection speed tends to be quite similar between the three mass flow rates when the distance from injection axis increases; at *2.5 mm* already, mass flow speeds are very close to each other.

Moreover, for the two highest mass flow rates presented in the graph above, it seems that passing from *1* to *2 mm*, they form a sort of hump in which their speed is even lower that that one with the lowest mass flow rate.

In the end, what it had been observed, is that, comparing speeds tested and speeds calculated, the difference between them is *10-20%*.

6.1.5   A particular case: *+75°*

During tests, once it was tried to test an injection angle of *+75°*, which was extremely positive, and very far from the optimal configuration; results are presented in Figure 42. Injection, in this case, works worse than what it had been obtained with other injection configurations; this could be explained quite simply saying that this type of injection works worse in the triangle of velocity, not pushing relative injection speed in the axial direction but on the other, opposite, direction. This causes a detrimental effect to compressor's

characteristic curve worsen it; *delta p* significantly decreases, and rotating stall is reached before, at higher mass flow rate.
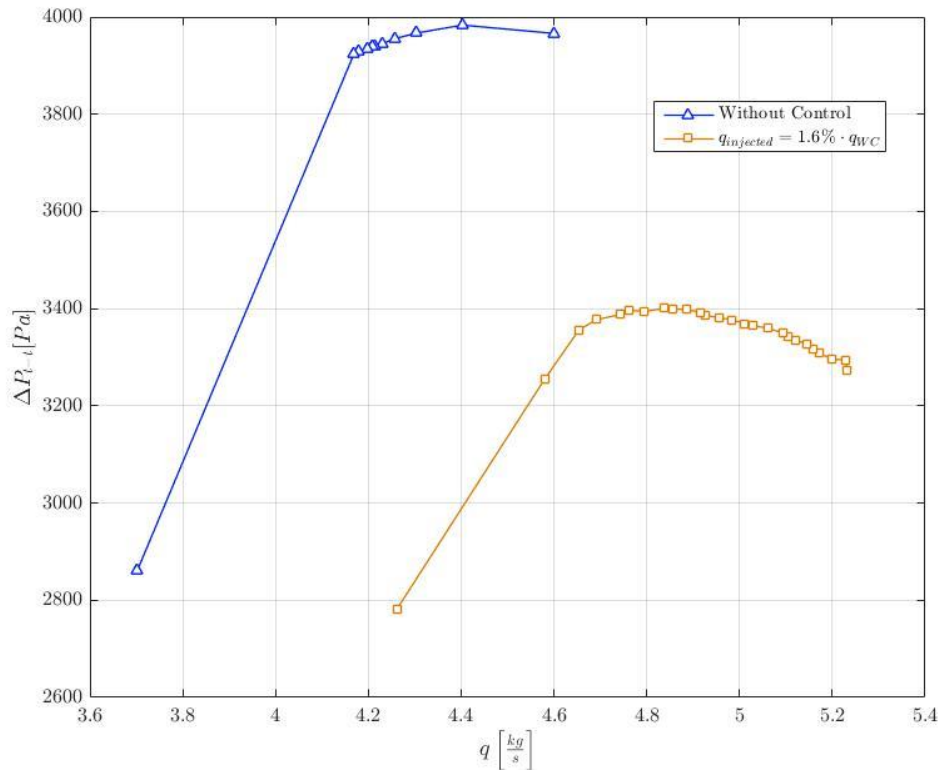

Figure 42: A particular case: +75° injection angle at 4 bar

6.2 PRESSURE BEHAVIOUR INSIDE ROTOR STAGE

In this section, pressure trend of the best configuration, *-30°*, is presented for the different injection pressure tested.

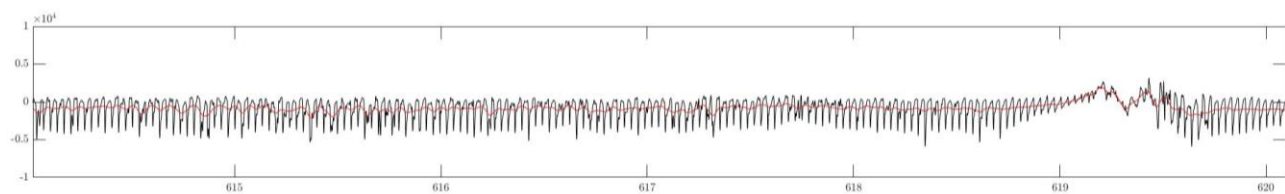### 6.2.1 *1-3-5-7 bar* injection pressure for *20 blocks* on

Figure 43: first probe pressure trend, approaching rotating stall for 1 bar injection

Figure 43 presents the unfiltered (in black) and filtered (in red) pressure trend for an injection pressure of *1 bar* as a function of the rotor revolutions. Rotating stall appears between *619* and *620 RPM* but there's no clear evidence of bump presence as a warning. There are only some perturbations ending *2* rotations before rotating stall appearance, but they cannot be considered as advice of it.
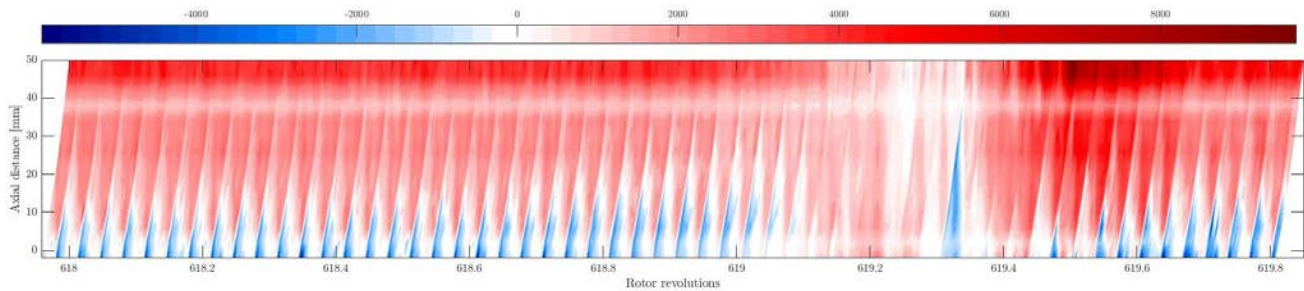

Figure 44: Pressure colormap approaching rotating stall for 1 bar injection

Looking at the colour map here above, it's possible to see the pressures field in rotor blades; each blade is not drawn in the graph, but they are placed just attached, on the left side, at those blue stripes on the lower part of the graph. Those blue stripes are the signature of low pressure, and, indeed they are placed just behind, on the rear part of the blades, close to the leading edge. Looking at them, it's clearly visible, they are increasing their length when approaching rotating stall; this because the triangle of velocity at leading edge is changing. This is due to the fact that mass flow rate sucked by compressor is decreasing and this means that incidence angle is increasing; this causes recirculation and vortexes in the zone immediately behind the blade. Injection jet is able to push them downstream and so avoid compressor reaching rotating stall. But when incidence angle is too high and the injection jet is no more able to maintain it under control, compressor goes into rotating. This is characterized by a zone of high pressures, placed at *619.2 RPM*, where blades are overload, and a zone of low ones, at almost *619.3 RPM*, where blades are unloaded.
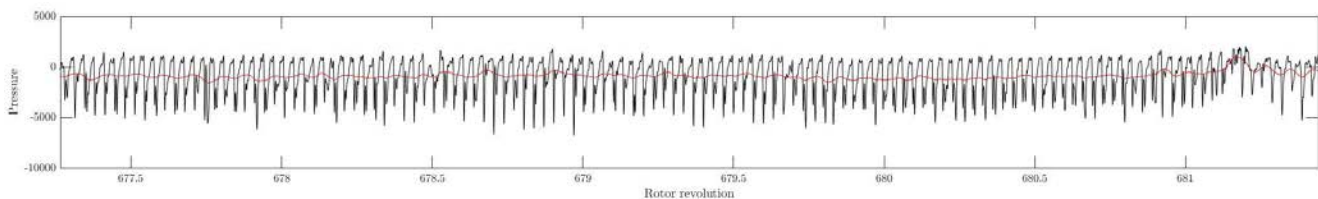

Figure 45: first probe pressure trend, approaching rotating stall for 3 bar injection

In the case of *3 bar* injection, there's a clear evidence of a bump when approaching rotating stall at almost *681 RPM*, but the pressure fluctuation is not so evident.
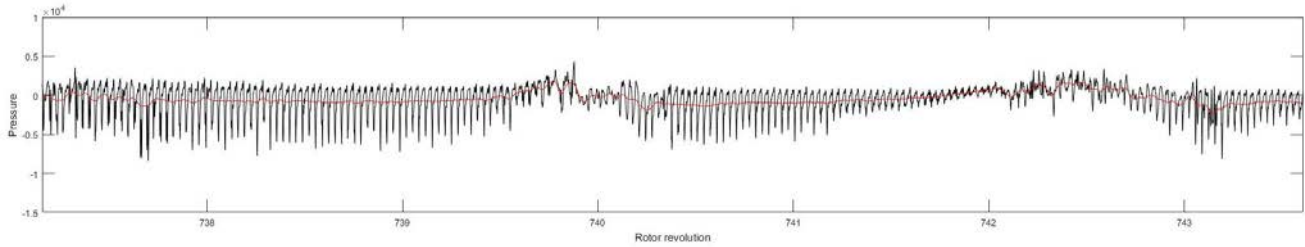
Figure 46: first probe pressure trend, approaching rotating stall for 5 bar injection
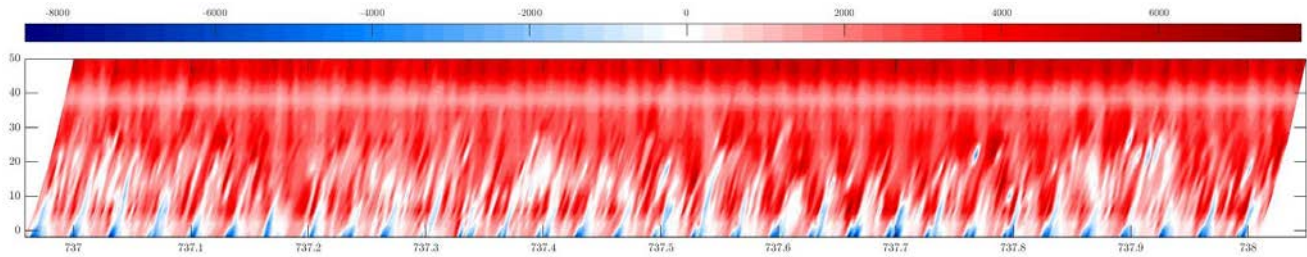

Figure 47: Pressure colour map approaching rotating stall for 5 bar injection

Looking at the case of *5 bar* injection in Figure 46, there isn't any clear evidence of the incoming of rotating stall, just some small bumps; if looking at Figure 47, there are some small signals of it. Firstly, it seems to be a light overpressure close to *737.1 RPM* and at *737.3 RPM* and secondly, contemporary, there are many vortexes traces throughout the snapshot taken: at from *737.3* up to *738 RPM*.

Anyway, if Figure 43 is compared with Figure 45 and Figure 46, looking at the y-axes scale intensity, it's possible to see that increasing injection pressure, the pressure warning tends to be higher in intensity; this could be explained thinking that, when injection pressure increases, the compressor goes into stall at lower mass flow rate, and this means that instabilities and perturbations are much more intense.
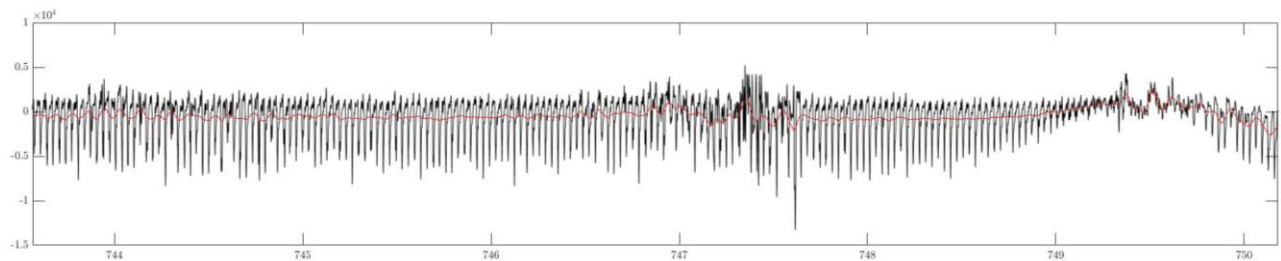

Figure 48: first probe pressure trend, approaching rotating stall for 7 bar injection
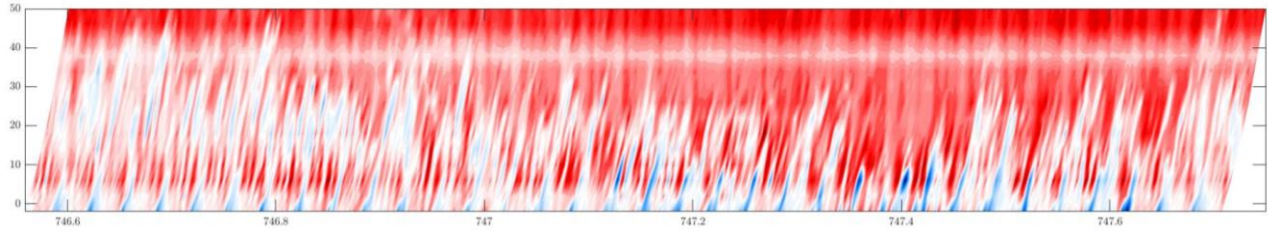
Figure 49: Pressure colour map approaching rotating stall for 7 bar injection

Concerning *7 bar* injection pressure, there clear traces of the incoming of rotating stall; looking at Figure 48 there are several bumps appearing before rotating stall appearance. Looking at when they happen, it's possible to see that rotating stall appears between *749* and *750 RPM* and the first and second warnings respectively at *744-745 RPM* and *747-748 RPM*. It is known that rotating stall used to propagate at *40/50%* rotational speed; this means that, for sure, these two disturbances are compressor's warnings of the rotating stall incoming.

In Figure 49, pressure colour map presents the pressure behaviour for the second rotating stall warning. There are clearly visible long, slight, blue coloured, tongues, starting from the leading edge and ending over the half of blades length. Some of them, especially in the right side of the graph, are particularly intense; it is very conceivable to think that they could be a vortexes' traces, that ones leading to recirculation and rotating stall.

6.2.2   *5-10-15 blocks* **on for *7 bar* injection pressure**

Here are presented graphs concerning different injector configurations and *7 bar* injection. Regarding *5 blocks* on configuration, looking at Figure 50, there are some heavy perturbations more or less *2* revolutions before rotating stall appearances, while a light one appears more or less *4* revolutions before it.
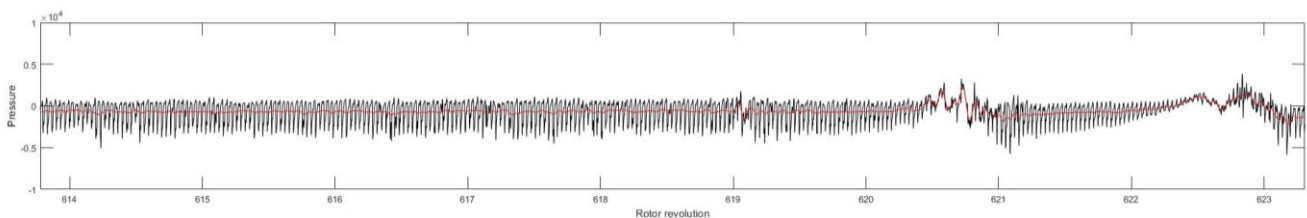

Figure 50: first probe pressure trend, approaching rotating stall for 7 bar injection and 5 blocks on
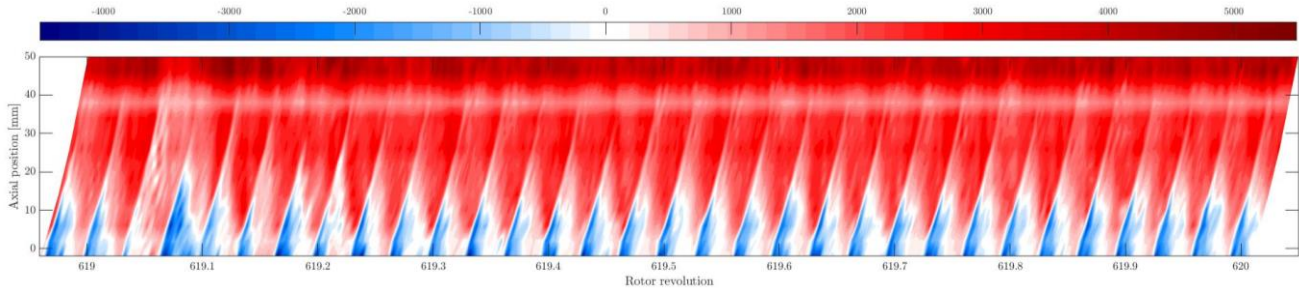
Figure 51: pressure colour map approaching rotating stall for 7 bar injection and 5 blocks on

Having a look at the colour map of Figure 51, what is really interesting to notice is that the very first warning appearing in this configuration is really well defined; close to *619.1 RPM* a blade pitch is completely blocked by recirculation. Figure clearly shows the very low pressure in the blade leading edge which covers the whole space between two consecutive blades; here, any mass flow rate will pass. Moreover, it will spread and lead to rotating stall.

For *10 blocks* injection on, presented in Figure 52 disturbances preceding rotating stall are very significant and high. Particularly, there are three different warning zones: the first one between *714* and *715 RPM*, the second one between *717* and *718 RPM* and finally the last one between *720* and *721 RPM*. All of them are spaced almost *2 RPM* one from the others.

Figure 52: first probe pressure trend, approaching rotating stall for 7 bar injection and 10 blocks on
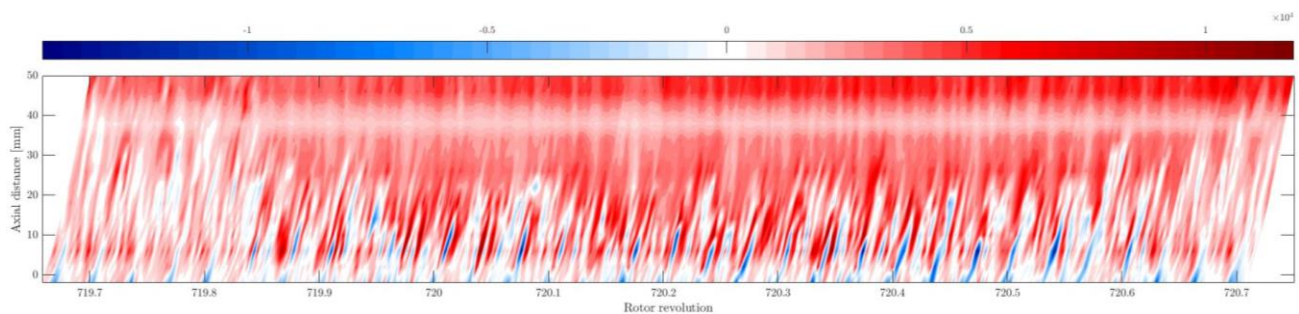
Figure 53: pressure colourmap approaching rotating stall for 7 bar injection and 10 blocks on

79

Finally, there's the case of *15 injection blocks* on presented below. Also here there's a big warning just *2 RPM* before rotating stall, at around *750 RPM*, and nothing else before; anyway, looking at the colour map in Figure 55, it's clear that this is not an advise of rotating stall, but it's already in rotating stall, because there are some blade's pitch that are overloaded and immediately after some other which are unloaded. So, it seems quite strange not to have any clear advice of rotating stall.
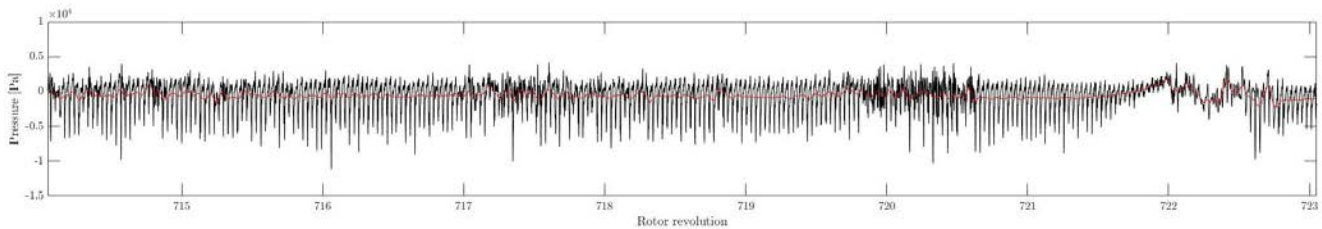

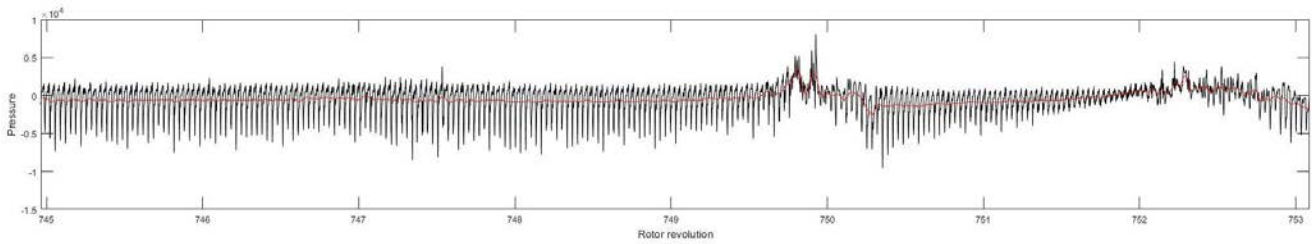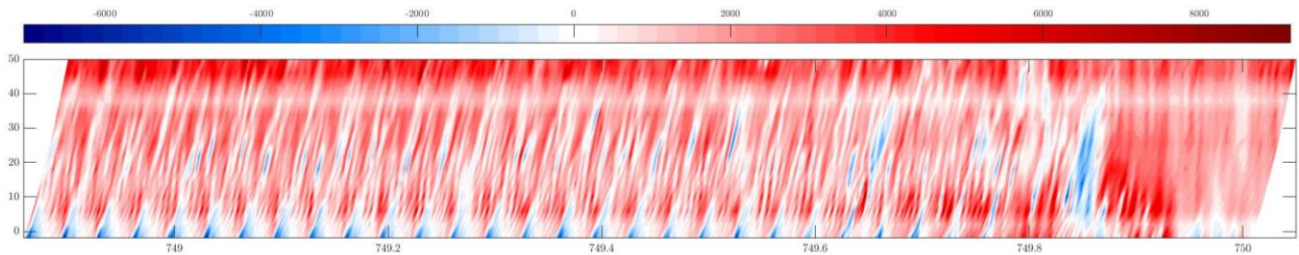*Figure 54: first probe pressure trend, approaching rotating stall for 7 bar injection and 15 blocks on*

Figure 55: pressure colourmap approaching rotating stall for 7 bar injection and 15 blocks on

7 CONCLUSIONS

This study reveals that the best injection angle configuration is *-30°* if injectors are all blowing, for any kind of injection pressure tested; anyway, the particularity of the configuration is that injectors position can be changed only by step of *15°*. This means that probably, what was found isn't the best injection configuration at all, but probably it is closest to it. Looking at Figure 30 and Figure 31, they confirm what has been said. Concerning the best injection configuration when injection pressure is kept constant, the best injection configuration, still remains *-30°* as Figure 32 shows. When injector configuration is fixed and injection pressure is varied, the best configuration is, again, *-30°* for each test pressure done. When pressure is fixed and number of injectors varied, the best injection angle is *-30°* only for higher number of injectors on; for lower numbers, like *5* or *8* the best solution is *-15°*.

This is explained because if the injection pressure is kept constant, reducing the injectors number that are blowing, increases the injection speed and so momentum injected, while, keeping constant the injectors number, the solution more affective is that one with the increasing of injection pressure, because this, as explained before, increases the momentum injected.

Concerning the energy balance, estimates on the speed evaluation shows that energy balance is always negative; this means that the stability improvement given by injection system isn't compensated by the increasing performances the compressor reaches. Bigger is the injection pressure and more negative is the energy balance.

Warnings appearing before rotating stall shows that they increase their intensity when injection pressure is increased; moreover, it seems that for low injection pressure there's only one advice before the appearing of rotating stall, while increasing the injection pressure, there are two warnings of its incoming. This is related to the fact that, with the same injectors configurations, the injection velocity, and so the momentum injected is higher and this stabilize more the compressor that can reduce more the mass flow rate sucked; by doing so, anyway, it is increasing instabilities and disturbances which at the beginning are compensated by the active control, but reducing more, they increase and injection system, at a certain point, is no more able to avoid the compressor to reach rotating stall.

On the last part, when the injection pressure is fixed, there are essentially no warning for *15 blocks* layout, while there are at least two of them for *5* and *10 blocks*.

What is common between all these types of solutions is that one or more warnings are appearing approximately two revolutions before rotating stall and there's the same distance between two or more consecutive warnings; this could lead to think that compressor is going to rotating stall through the modes and not spikes.

8 FUTURE PERSPECTIVE

There are still plenty of work to do to understand better how to be able to predict rotating stall, how it evolves and how it can be extinguished.

As it was reported in the conclusions, the best configuration founded for the specific configuration is not so precise because injection angle step was of *15°*; so, it would be better to have, at least, a sensibility of a couple of degrees in order to find more precisely the best injection angle configuration.

Another important thing to do is to study and build up a mathematical model to calculate, for each compressor, and its configuration, the exact point at which it will go into rotating stall; this is obviously the best scenario, but it will for sure helps researcher to make a big step forward in this research field.

Particularly, it will be very important to analytically understand how injection velocity and injection momentum will affect rotating stall; in this work, the two major limits were: not being able to evaluate exit velocity and not being able to describe through equations what's happening inside the compressor. This is for sure not simple as the problem faced was a 3D one, but maybe some other important aspect could be evaluated.

Then, what would help again is Computational Fluid Dynamics analysis; making several CFD analysis around several different configuration will surely help to understand how phenomenon evolves.

Important and several studies could be done on injectors; which is the best layout for each of them (for example if there's a best width and thickness for the jet), which is the best axial position where to place them and also the radial one.

Finally, it would be amazing to build up a program which activates injectors only when they are necessary, just a couple of rotation before rotating stall; furthermore, it would be better to project the system in order to activate not simply all injectors, but only those ones which are necessary to avoid compressor entering rotating stall.

9 REFERENCES

Beheshti, B. H., Ghorbanian, K., Farhanieh, B., Teixeira, J. A., & Ivey, P. C. (2008). *A New Design for Tip Injection in Transonic Axial Compressors*. 39–47. https://doi.org/10.1115/gt2006-90007

Behnken, R. L. (1997). Rotating Stall Control of an Axial Flow Compressor Using Pulsed Air Injection. *Journal of Turbomachinery*, *119*(4), 742. https://doi.org/10.1115/1.2841184

Boyce, M. P. (2012). *Gas Turbine Engineering Handbook* (Fourth; Elsevier, ed.).

Day, I. J. (2015). Stall, Surge, and 75 Years of Research. *Journal of Turbomachinery*, *138*(1), 011001. https://doi.org/10.1115/1.4031473

Greitzer, E. M. (1976a). Surge and Rotating Stall in Axial Flow Compressors—Part II: Experimental Results and Comparison With Theory. *Journal of Engineering for Power*, *98*(2), 199. https://doi.org/10.1115/1.3446139

Greitzer, E. M. (1976b). Surge and rotating stall in axial flow compressors: Part I: Theoretical compression system model. *Journal of Engineering for Gas Turbines and Power*, *98*(2), 190–198. https://doi.org/10.1115/1.3446138

Guinet, C., Inzenhofer, A., & Gümmer, V. (2016). Influencing Parameters of Tip Blowing Interacting With Rotor Tip Flow. *Journal of Turbomachinery*, *139*(2), 021010. https://doi.org/10.1115/1.4034699

Hewkin-Smith, M., Pullan, G., Grimshaw, S. D., Greitzer, E. M., & Spakovszky, Z. S. (2019). The Role of Tip Leakage Flow in Spike-Type Rotating Stall Inception. *Volume 2D: Turbomachinery*, *141*(June), V02DT46A009. https://doi.org/10.1115/GT2017-63655

Kefalakis, M., & Papailiou, K. D. (2007). Axial compressor stage detailed measurements with application of discrete tip injection to increase surge margin. *Proceedings of the 7th European Conference on Turbomachinery: Fluid Dynamics and Thermodynamics, ETC 2007*, (August).

Kefalakis, M., & Papailiou, K. D. (2008). *Active Flow Control for Increasing the Surge Margin of an Axial Flow Compressor*. 101–111. https://doi.org/10.1115/gt2006-90113

Khaleghi, H., Dehkordi, M. A. S., & Tousi, A. M. (2016). Role of tip injection in desensitizing the compressor to the tip clearance size. *Aerospace Science and Technology*, *52*, 10–17. https://doi.org/10.1016/j.ast.2016.02.003

Khaleghi, H., Teixeira, J. A., Tousi, A. M., & Boroomand, M. (2008). Parametric Study of Injection Angle Effects on Stability Enhancement of Transonic Axial Compressors. *Journal of Propulsion and Power*, *24*(5), 1100–1107. https://doi.org/10.2514/1.34817

Li, J., Du, J., Nie, C., & Zhang, H. (2019). Review of tip air injection to improve stall margin in axial compressors. *Progress in Aerospace Sciences*, *106*(October 2018), 15–31. https://doi.org/10.1016/j.paerosci.2019.01.005

Li, J., Lin, F., Tong, Z., Nie, C., & Chen, J. (2014). The Dual Mechanisms and Implementations of Stability Enhancement With Discrete Tip Injection in Axial Flow Compressors. *Journal of Turbomachinery*, *137*(3), 031010. https://doi.org/10.1115/1.4028299

Liu, X., Teng, J., Yang, J., Sun, X., Sun, D., He, C., & Du, J. (2019). Calculation of Stall Margin Enhancement With Micro-Tip Injection in an Axial Compressor. *Journal of Fluids Engineering*, *141*(8), 081109. https://doi.org/10.1115/1.4042561

Lu, X., Chu, W., Zhu, J., & Tong, Z. (2006). Numerical and Experimental Investigations of Steady Micro-Tip Injection on a Subsonic Axial-Flow Compressor Rotor. *International Journal of Rotating Machinery*, *2006*, 1–11. https://doi.org/10.1155/ijrm/2006/71034

Mushtaq, A., Parvez, K., Ahmad, S., & Khan, J. (2012). *Parametric Study of Tip Injection on Stability of Transonic Axial Flow Compressor*. 1–9. https://doi.org/10.2514/6.2011-744

Nie, C., Tong, Z., Geng, S., Zhu, J., & Huang, W. (2007). Experimental investigations of micro air injection to control rotating stall. *Journal of Thermal Science*, *16*(1), 1–6. https://doi.org/10.1007/s11630-007-0001-x

Nie, C., Xu, G., Cheng, X., & Chen, J. (2002). Micro Air Injection and Its Unsteady Response in a Low-Speed Axial Compressor. *Journal of Turbomachinery*, *124*(4), 572. https://doi.org/10.1115/1.1508383

Pullan, G., Young, A. M., Day, I. J., Greitzer, E. M., & Spakovszky, Z. S. (2012). Origins and Structure of Spike-Type Rotating Stall. *Volume 8: Turbomachinery, Parts A, B, and C*, *137*(May 2015), 2567. https://doi.org/10.1115/GT2012-68707

Salunkhe, P. B., Reddy, V. S. R. K., & Pradeep, A. M. (2009). Tip injection as a means for rotating stall control in an axial flow fan. *Proceedings of the Institution of Mechanical Engineers, Part A: Journal of Power and Energy*, *223*(1), 55–70. https://doi.org/10.1243/09576509JPE646

Suder, K. L., Hathaway, M. D., Thorp, S. A., Strazisar, A. J., & Bright, M. B. (2002). Compressor Stability

Enhancement Using Discrete Tip Injection. *Journal of Turbomachinery*, *123*(1), 14. https://doi.org/10.1115/1.1330272

Taghavi-Zenouz, R., & Ababaf Behbahani, M. H. (2018). Improvement of aerodynamic performance of a low speed axial compressor rotor blade row through air injection. *Aerospace Science and Technology*, *72*, 409–417. https://doi.org/10.1016/j.ast.2017.11.028

WANG, W., CHU, W., ZHANG, H., & KUANG, H. (2017). Experimental and numerical study of tip injection in a subsonic axial flow compressor. *Chinese Journal of Aeronautics*, *30*(3), 907–917. https://doi.org/10.1016/j.cja.2017.04.004

10 APPENDIX

Here we report all Matlab files used for the data processing, graphs creations and comparisons.

- "traitement_soufflage_bis":

  file:///E:/Thesis/Traitment%20soufflage/html/traitement_soufflage_bis.html

- "Super_programma":

  file:///E:/Thesis/Test%20sperimentali/Confronto/Tutto/html/Super_programma.html

- "interface_bis":

  file:///E:/Thesis/Analysis%20GUI/html/interface_bis.html